Westinghouse

Westinghouse Electric Company
Nuclear Power Plants
P.O. Box 355
Pittsburgh, Pennsylvania 15230-0355
USA

U.S. Nuclear Regulatory Commission
ATTENTION: Document Control Desk
Washington, D.C. 20555

Direct tel: 412-374-6206
Direct fax: 412-374-5005
e-mail: sisk1rb@westinghouse.com

Your ref: Docket Number 52-006
Our ref: DCP/NRC2130

May 2, 2008

Subject: AP1000 Standard COL Technical Report Submittal of APP-GW-GLR-033, Revision 1 (TR 54)

In support of the On-Site Technical Review meeting on seismic and structural issues scheduled for the week of May 19, 2008, Westinghouse is submitting Revision 1 of AP1000 Standard Combined License Technical Report Number 54, "Spent Fuel Storage Rack Structure/Seismic Analysis." The purpose of Technical Report 54 (TR 54) is to complete and document, on a generic basis, activities required for COL Information Item 9.1-3 in the AP1000 Design Control Document (DCD). This revision to Technical Report 54 incorporates changes made in response to NRC Requests for Additional Information (RAI) and in response to feedback received from the NRC during the October 2007 Audit. The proposed changes included in this revision are changes to Revision 16 of the AP1000 DCD and do not include changes previously submitted in Revision 0 of this report.

This report is submitted in support of the AP1000 Design Certification Amendment Application (Docket No. 52-006). The information provided in this report is generic and is expected to apply to all Combined Operating License (COL) applicants referencing the AP1000 Design Certification and the AP1000 Design Certification Amendment Application.

Pursuant to 10 CFR 50.30(b), APP-GW-GLR-033, Revision 1, "Spent Fuel Storage Rack Structure/Seismic Analysis," Technical Report Number 54 is submitted as Enclosure 1 under the attached Oath of Affirmation. Revision 0 of TR 54 was submitted under Westinghouse letter DCP/NRC1760, dated July 7, 2006.

Questions or requests for additional information related to the content and preparation of this report should be directed to Westinghouse. Please send copies of such questions or requests to the prospective applicants for combined licenses referencing the AP1000 Design Certification. A representative for each applicant is included on the cc: list of this letter.

Very truly yours,

R. B. Sisk, Manager
Licensing and Customer Interface
Regulatory Affairs and Standardization

D063
NRO

00369psa.doc

/Attachment

1. "Oath of Affirmation," dated May 2, 2008

/Enclosure

1. APP-GW-GLR-033, Revision 1, "Spent Fuel Storage Rack Structure/Seismic Analysis," Technical Report Number 54

cc:	M. Miernicki	-	U.S. NRC	1E	1A
	E. McKenna	-	U.S. NRC	1E	1A
	P. Ray	-	TVA	1E	1A
	P. Hastings	-	Duke Power	1E	1A
	R. Kitchen	-	Progress Energy	1E	1A
	A. Monroe	-	SCANA	1E	1A
	J. Wilkinson	-	Florida Power & Light	1E	1A
	C. Pierce	-	Southern Company	1E	1A
	G. Zinke	-	NuStart/Entergy	1E	1A
	R. Grumbir	-	NuStart	1E	1A
	E. Schmiech	-	Westinghouse	1E	1A
	J. Iacovino	-	Westinghouse	1E	1A

ATTACHMENT 1

"Oath of Affirmation"

ATTACHMENT 1

UNITED STATES OF AMERICA

NUCLEAR REGULATORY COMMISSION

In the Matter of:)

AP1000 Design Certification Amendment Application)

NRC Docket Number 52-006)

APPLICATION FOR REVIEW OF
"AP1000 GENERAL INFORMATION"
FOR AP1000 DESIGN CERTIFICATION AMENDMENT APPLICATION REVIEW

W. E. Cummins, being duly sworn, states that he is Vice President, Regulatory Affairs and Standardization, for Westinghouse Electric Company; that he is authorized on the part of said company to sign and file with the Nuclear Regulatory Commission this document; that all statements made and matters set forth therein are true and correct to the best of his knowledge, information and belief.

W. E. Cummins
Vice President
Regulatory Affairs and Standardization

Subscribed and sworn to
before me this 2nd day
of May 2008.

COMMONWEALTH OF PENNSYLVANIA
Notarial Seal
Patricia S. Aston, Notary Public
Murrysville Boro, Westmoreland County
My Commission Expires July 11, 2011
Member, Pennsylvania Association of Notaries

Notary Public

ENCLOSURE 1

APP-GW-GLR-033

Revision 1

"Spent Fuel Storage Rack Structure/Seismic Analysis"

Technical Report Number 54

F-AP-3.2-1 Rev 4

AP1000 DOCUMENT COVER SHEET

TDC: _____ Permanent File: _____

AP1000 DOCUMENT NO.	REVISION	PAGE	ASSIGNED TO	OPEN ITEMS (Y/N)
APP-GW-GLR-033	1	1 of ~~78~~ 69	W-D. Ekeroth	N

ALTERNATE DOCUMENT NUMBER: TR54 WORK BREAKDOWN #: 1.6.4.5.15

ORIGINATING ORGANIZATION: Westinghouse Electric Company

TITLE: **Spent Fuel Storage Racks Structure/Seismic Analysis**

ATTACHMENTS:	DCP #/REV. INCORPORATED IN THIS DOCUMENT REVISION:
None	APP-GW-GEE-068, Rev. 3
CALCULATION/ANALYSIS REFERENCE: APP-FS02-S3C-002 Rev. 1	APP-GW-GEE-112, Rev. 0

ELECTRONIC FILENAME	ELECTRONIC FILE FORMAT	ELECTRONIC FILE DESCRIPTION
APP-GW-GLR-033R1.doc	Microsoft Word	Text

☒ **© 2008 WESTINGHOUSE ELECTRIC COMPANY LLC – WESTINGHOUSE NON-PROPRIETARY CLASS 3**

Class 3 Documents being transmitted to the NRC require the following two review signatures in lieu of a Form 36.

LEGAL REVIEW T. J. White	SIGNATURE / DATE (If processing electronic approval select option) T. J. White 5-1-08
PATENT REVIEW ~~F. L. Carpentino~~ Douglas Ekeroth 4/30/08	SIGNATURE / DATE Douglas E Ekeroth 4/30/08

☐ **© 2008 WESTINGHOUSE ELECTRIC COMPANY LLC – WESTINGHOUSE PROPRIETARY CLASS 2**

This document is the property of and contains Proprietary Information owned by Westinghouse Electric Company LLC and/or its subcontractors and suppliers. It is transmitted to you in confidence and trust, and you agree to treat this document in strict accordance with the terms and conditions of the agreement under which it was provided to you.

☐ **© 2008 WESTINGHOUSE ELECTRIC COMPANY LLC and/or STONE & WEBSTER, INC.**

WESTINGHOUSE PROPRIETARY CLASS 2 and/or STONE & WEBSTER CONFIDENTIAL AND PROPRIETARY

This document is the property of and contains Proprietary Information owned by Westinghouse Electric Company LLC and/or is the property of and contains Confidential and Proprietary Information owned by Stone & Webster, Inc. and/or their affiliates, subcontractors and suppliers. It is transmitted to you in confidence and trust, and you agree to treat this document in strict accordance with the terms and conditions of the agreement under which it was provided to you.

ORIGINATOR(S) J. M. Iacovino Jr.	SIGNATURE / DATE (If processing electronic approval select option) (signed) JM IACOVINO JR 4-30-08	
REVIEWER(S) M. McCullough	SIGNATURE / DATE 4-30-08	
	SIGNATURE / DATE	
	SIGNATURE / DATE	
VERIFIER(S) J. Fernandez	SIGNATURE / DATE 5/2/08	Verification Method: Independent Review

**Plant Applicability: ☑ All AP1000 plants except: None
☐ Only the following plants:

APPLICABILITY REVIEWER** J. A. Speer	SIGNATURE / DATE 5/1/08
RESPONSIBLE MANAGER* D. Ekeroth	SIGNATURE / DATE 5/2/08

* Approval of the responsible manager signifies that the document and all required reviews are complete, the appropriate proprietary class has been assigned, electronic file has been provided to the EDMS, and the document is released for use.

*** *Electronically approved records are authenticated in the electronic document management system.*

AP1000 Standard Combined License Technical Report

Spent Fuel Storage Racks Structural/Seismic Analysis

Westinghouse Electric Company LLC
P.O. Box 355
Pittsburgh, PA 15230-0355

© 2008 Westinghouse Electric Company LLC
All Rights Reserved

TABLE OF CONTENTS

LIST OF TABLES ii
LIST OF FIGURES iii

1 INTRODUCTION 1

2 TECHNICAL BACKGROUND 1
2.1 DESIGN 2
2.1.1 AP1000 Spent Fuel Storage Racks Description 2
2.2 METHODOLOGY 4
2.2.1 Acceleration Time Histories 4
2.2.2 Modeling Methodology 4
2.2.3 Simulation and Solution Methodology 8
2.2.4 Conservatisms Inherent in Methodology 9
2.3 KINEMATIC AND STRESS ACCEPTANCE CRITERIA 9
2.3.1 Introduction 9
2.3.2 Kinematic Criteria 9
2.3.3 Stress Limit Criteria 10
2.3.4 Stress Limits for Various Conditions Per ASME Code 10
2.3.5 Dimensionless Stress Factors 13
2.4 ASSUMPTIONS 14
2.5 INPUT DATA 14
2.5.1 Rack Data 14
2.5.2 Structural Damping 14
2.5.3 Material Data 14
2.6 COMPUTER CODES 14
2.7 ANALYSES 14
2.7.1 Acceptance Criteria 14
2.7.2 Dynamic Simulations 15
2.8 RESULTS OF ANALYSES 15
2.8.1 Time History Simulation Results 15
2.8.2 Rack Structural Evaluation 16
2.8.3 Dead Load Evaluation 18
2.8.4 Local Stress Considerations 19
2.8.5 Hypothetical Fuel Assembly Drop Accidents 21
2.8.6 Stuck Fuel Assembly Evaluation 22
2.9 CONCLUSIONS 23

3 REGULATORY IMPACT 52

4 REFERENCES 52

5 DCD MARKUP 54

LIST OF TABLES

Table 2-1 Region 1 Storage Racks 24
Table 2-2 Region 2 Spent Fuel Pool Storage Racks 25
Table 2-3 Spent Fuel Pool Damaged Fuel Assembly Storage Cells 26
Table 2-4 Simulation Listing 27
Table 2-5 Loading Combinations for AP1000 Spent Fuel Storage Racks 27
Table 2-6 Material Data (ASME – Section II, Part D) 28
Table 2-7 AP1000 Spent Fuel Storage Racks and Fuel Data 29
Table 2-8 Computer Codes Used for AP1000 Spent Fuel Storage Racks Structural/Seismic Analysis 30
Table 2-9 Results Summary 31
Table 2-10 Time History Post-Processor Results 31
Table 2-11 Maximum Stress Factors 32
Table 2-12 Baseplate-to-Cell Maximum Weld Stress 33
Table 2-13 Base Metal Shear Stress at Baseplate-to-Cell Weld Location 33
Table 2-14 Baseplate-to-Pedestal Welds 33
Table 2-15 Pedestal Thread Shear Stress 33
Table 2-16 Maximum Cell-to-Cell Weld Stress 33
Table 2-17 Maximum Base Metal Shear Stress at Cell-to-Cell Weld Location 34
Table 2-18 Degrees of Freedom for Single Rack Dynamic Model 34
Table 2-19 Results from Stuck Fuel Assembly Evaluation 35

LIST OF FIGURES

Figure 2-1 Spent Fuel Pool Storage Layout (889 Total Storage Locations) – Leak Chases Show in Phantom 36
Figure 2-2 Configuration of a Region 1 Storage Cell (Sheet 1 of 2) 37
Figure 2-2 Configuration of a Region 1 Storage Cell (Sheet 2 of 2) 38
Figure 2-3 Configuration of a Region 2 Storage Cell (Sheet 1 of 2) 39
Figure 2-3 Configuration of a Region 2 Storage Cell (Sheet 2 of 2) 40
Figure 2-4 Schematic Diagram of Dynamic Model for DYNARACK 41
Figure 2-5 Rack-to-Rack Impact Springs 42
Figure 2-6 Fuel-to-Rack Impact Springs at Level of Rattling Mass 43
Figure 2-7 Two-Dimensional View of Spring-Mass Simulation 44
Figure 2-8 Rack Degrees-of-Freedom for X-Y Plane Bending with Shear and Bending Spring 45
Figure 2-9 LS-DYNA Model of Dropped Fuel Assembly 46
Figure 2-10 LS-DYNA Model of Top and Bottom of AP1000 Region 1 Spent Fuel Rack 47
Figure 2-11 LS-DYNA Model of Top and Bottom of AP1000 Region 2 Spent Fuel Rack 48
Figure 2-12 Plastic Strain Results from Drop to Top of Region 2 Spent Fuel Rack 49
Figure 2-13 Maximum Rack Baseplate Deformation from Drop into an Empty Cell (One-Quarter of Impact Zone Shown) 50
Figure 2-14 Plastic Strain in Pool Liner from Drop over Rack Pedestal 51
Figure 9.1-2 (Sheet 1 of 2)Region 1 Spent Fuel Storage Rack Layout 56
Figure 9.1-2 (Sheet 2 of 2) Region 1 Spent Fuel Storage Rack Cross Section 58
Figure 9.1-3 (Sheet 1 of 2) Region 2 Spent Fuel Storage Rack Layout 60
Figure 9.1-3 (Sheet 2 of 2) Region 2 Spent Fuel Storage Rack Cross Section 62
Figure 9.1-4 Spent Fuel Storage Pool Layout (889 Storage Locations) 64

1 INTRODUCTION

This report summarizes the structural/seismic analysis of the AP1000 Spent Fuel Storage Racks. This revision specifically addresses Westinghouse responses to U.S. Nuclear Regulatory Commission (U.S. NRC) Requests for Additional Information (RAIs). The AP1000 Spent Fuel Storage Racks are used to store fresh fuel assemblies prior to loading them in the reactor core and spent fuel assemblies after they have been discharged from the reactor core. The requirements for this analysis are identified in the AP1000 Design Control Document (DCD), subsection 9.1.2.2.1 (Reference 1). The completion of this analysis is identified as Combined Operating License (COL) Information Item 9.1-3 (Final Safety Evaluation Report [Reference 2] Action Item 9.1.6-3) in DCD subsection 9.1.6 to be completed by the Combined License applicant.

> COL Information Item 9.1-3: "Perform a confirmatory structural dynamic and stress analysis for the spent fuel rack, as described in subsection 9.1.2.2.1." This includes reconciliation of loads imposed by the spent fuel rack on the spent fuel pool structure described in subsection 3.8.4."

This COLA Technical Report specifically addresses the first sentence of COL Information Item 9.1-3. The calculation "AP1000 Spent Fuel Storage Racks Structural/Seismic Analysis" (Reference 3) is available for U.S. NRC audit. A summary of the criticality analysis for the AP1000 Spent Fuel Storage Racks is presented in AP1000 Standard Combined License Technical Report, "Spent Fuel Storage Racks Criticality Analysis" (Reference 4). The reconciliation of loads imposed by the spent fuel racks on the spent pool structure described in subsection 3.8.4 is provided in calculation, "Design of Spent Fuel Pit Floor in Module CA20," Reference 27). The conclusion of this calculation is that the design of the fuel pool floor is adequate with respect to the loadings of completely filled spent fuel racks.

This report also documents changes to the spent fuel racks to hold a larger number of fuel assemblies. The descriptions of the AP1000 Spent Fuel Storage Racks and analysis, as discussed in DCD subsection 9.1.2, "Spent Fuel Storage," and general arrangement, as discussed in DCD Section 1.2, "General Plant Description," of Reference 1, are updated to reflect the changes in the spent fuel racks and their capacity to hold a greater number of fuel assemblies.

2 TECHNICAL BACKGROUND

This report considers the structural adequacy of the proposed AP1000 Spent Fuel Storage Racks under postulated loading conditions. Analyses and evaluations follow the U.S. Office of Technology Position Paper (Reference 5) and the U.S. NRC Standard Review Plan (Reference 6), whichever is more limiting. The dynamic analyses use a time-history simulation code used in numerous previous licensing efforts in the United States and abroad. This report provides a discussion of the method of analyses, modeling assumptions, key evaluations, and results obtained to establish the margins of safety.

2.1 DESIGN

2.1.1 AP1000 Spent Fuel Storage Racks Description

Figure 2-1 presents the layout of the AP1000 spent fuel pool. The updated total storage capacity is 889 locations. The AP1000 spent fuel pool contains three Region 1 rack modules and five Region 2 rack modules, one of which contains five Defective Fuel Assembly Storage Cells. The Spent Fuel Pool Cooling System has the capability to cool a fully loaded spent fuel pool under the design-basis conditions.

There are three Region 1 modules, which are all 9x9 arrays of storage cells. They are designated Modules A1, A2, and A3. Note that the Region 1 modules are located along the west wall of the AP1000 spent fuel pool. Region 1 racks are designed to hold fresh and spent fuel assemblies in accordance with Reference 4.

There are four Region 2 modules, which are 12x11 arrays of storage cells. The 12x11 modules are designated Modules B1, B2, B3, and B4. These modules are located along the east wall of the AP1000 spent fuel pool. These racks are designed to hold spent fuel assemblies in accordance with Reference 4.

There is a single 12x10 (-2) Region 2 module. It is designated Module C1. (Note that the term "12x10 (-2)" means a 12x10 array that is missing seven Region 2 storage cells. The seven storage cells removed from the 12x10 array provide space for the five Defective Fuel Assembly Storage Cells.) The five Defective Fuel Assembly Storage Cells are designed to hold fresh or spent fuel assemblies that are defective in accordance with Reference 4.

2.1.1.1 Region 1 Storage Cell Description

Figure 2-2 presents the configuration of a Region 1 storage cell. The Region 1 storage cells are centered on a pitch of 10.9 inches. Each storage cell consists of a stainless steel canister, which has a nominal inside dimension of 8.8 inches and is 0.075 inch thick. Metamic® panels are attached to the outside surfaces of the canister in all Region 1 storage cells except for the surfaces directly facing the west wall of the spent fuel pool. Each Metamic poison panel is held in place and is centered on the width of the stainless steel canister by an outer stainless steel sheathing panel. There is a small void space (nominally 0.012 inch) between the sheathing and the Metamic panel. The dimensions of the Metamic poison panel are 7.5 inches wide by 0.106 inch thick. The sheathing panels on interior storage canisters are 0.035 inch thick on the interior of the rack and 0.075 inch thick on the perimeter of the rack.

Each Region 1 storage cell is 199.5 inches long, and rests on top of a base plate whose top is 5 inches above the spent fuel pool liner floor. Note that each Metamic poison panel is 172 inches long and has a bottom elevation that is 6.23 inches above the top of the base plate. The bottom elevation of the Metamic poison panel was positioned to be 2 inches lower than the bottom elevation of the active fuel. The Metamic poison material is a mixture of B_4C and Al with a nominal B_4C concentration equal to 31.0 weight-percent, and uses natural boron isotopics (i.e., not enriched B^{10}). The Region 1 storage cell dimensions and tolerances are summarized in Table 2-1.

2.1.1.2 Region 2 Storage Cell Description

Figure 2-3 presents the configuration of a Region 2 Storage Cell. The Region 2 storage cells are formed by welding open stainless steel canisters together at the corners. Therefore, the Region 2 storage cells are a combination of individual canister storage cells and "developed" storage cells. The "developed" storage cells result from the welding process. As an example, the welding of four canisters at the corners of each canister produces a single "developed" storage cell at the center of the four canisters. Each Region 2 stainless steel canister has an inside dimension of 8.8 inches and is 0.075 inch thick. The center-to-center spacing between storage cells is 9.028 inches.

Metamic panels are attached to the outside surfaces of each stainless steel canister except for the surfaces directly facing the walls of the spent fuel pool. The exception is the C1 rack, where the Region 2 cells facing the west wall of the spent fuel pool have Metamic panels. Each Metamic poison panel is held in place and is centered on the width of the stainless steel canister by an outer stainless steel sheathing panel. There is a small void space (nominally 0.012 inch) between the sheathing and the Metamic panel. The dimensions of the Metamic poison panel are 7.5 inches wide by 0.106 inch thick. The sheathing panels on interior storage canisters are 0.035 inch thick on the interior of the rack and 0.075 inch thick on the perimeter of the rack.

Each Region 2 storage cell is 199.5 inches long, and rests on top of a base plate whose top is 5 inches above the spent fuel pool liner floor. Note that each Metamic poison panel is 172 inches long and has a bottom elevation that is 6.23 inches above the top of the base plate. The bottom elevation of the Metamic poison panel was positioned to be 2 inches lower than the bottom elevation of the active fuel. The Metamic poison material is a mixture of B_2C and Al with a nominal B_4C concentration equal to 31.0 weight-percent, and uses natural boron isotopics (i.e., not enriched B^{10}). The Region 2 storage cell dimensions are summarized in Table 2-2.

2.1.1.3 Defective Fuel Assembly Storage Cell

The Defective Fuel Assembly Storage Cells consist of open stainless canisters with an inside dimension of 10.25 inches and a thickness of 0.075 inch. The center-to-center spacing between storage cells is 10.478 inches. Metamic panels are attached to the surfaces of the canisters which face another canister or a Region 2 cell. Each Metamic poison panel is held in place and is centered on the width of the stainless steel canister by an outer stainless steel sheathing panel. There is a small void space (nominally 0.012 inch) between the sheathing and the Metamic panel. The dimensions of the Metamic poison panel are 7.5 inches wide by 0.106 inch thick. The sheathing panels on interior facing walls are 0.035 inch thick interior of the rack and 0.075 inch thick on the perimeter of the rack.

Each Defective Fuel Assembly Storage Cell is 199.5 inches long, and each rests on top of a base plate whose top is 5 inches above the spent fuel pool liner floor. Note that each Metamic poison panel is 172 inches long, and each has a bottom elevation that is 6.23 inches above the top of the base plate. The bottom elevation of the Metamic poison panel was positioned to be 2 inches lower than the bottom elevation of the active fuel. The Metamic poison material is a mixture of B_4C (31.0 weight-percent) and Al (69.0 weight-percent). The Defective Fuel Assembly Storage Cell dimensions are summarized in Table 2-3.

2.2 METHODOLOGY

2.2.1 Acceleration Time Histories

The response of a freestanding rack module to seismic inputs is highly nonlinear, and it involves a complex combination of motions (sliding, rocking, twisting, and turning), resulting in impacts and frictional effects. Linear methods, such as modal analysis and response spectrum techniques, cannot accurately replicate the response of such a highly nonlinear structure to seismic excitation. An accurate simulation is obtained only by direct integration of the nonlinear equations of motion using actual pool slab acceleration time-histories as the forcing function. Therefore, the initial step in AP1000 Spent Fuel Storage Racks qualification is to develop synthetic time-histories for three orthogonal directions, which comply with the guidelines of the U.S. NRC Standard Review Plan (Reference 8). In particular, the synthetic time-histories must meet the criteria of statistical independence, envelope the target design response spectra, and envelope the target Power Spectral Density function associated with the target response spectra. The acceleration time-histories for the ASB99 Floor Response Spectra (FRS) were developed in Reference 23. The ASB99 FRS were generated by Westinghouse in Reference 19. The ASB99 FRS represent the enveloping response spectra for the Auxiliary and Shield Building (ASB) at Elevation 99 feet for a range of soil/rock condition. FRS of various soil/rock analyses were first enveloped for various locations of the ASB. All of the ASB locations at Elevation 99 feet were then grouped and enveloped to develop the ASB99 floor response spectra. The spent fuel pool is at a lower elevation but the dynamic response is essentially the same as at Elevation 99 feet.

The acceleration time histories for the ASB99 FRS are used as the input motion for the seismic analysis of the spent fuel racks. The three orthogonal components are input and solved simultaneously.

2.2.2 Modeling Methodology

2.2.2.1 General Considerations

Once a set of input excitations is obtained, a dynamic representation is developed. Reliable assessment of the stress field and kinematic behavior of the rack modules calls for a conservative dynamic model incorporating all key attributes of the actual structure. This means that the dynamic model must have the ability to execute concurrent sliding, rocking, bending, twisting, and other motion forms compatible with the freestanding installation of the modules. Additionally, the model must possess the capability to effect momentum transfers that occur due to rattling of fuel assemblies inside storage cells and the capability to simulate lift-off and subsequent impact of support pedestals with the pool liner. The contribution of the water mass in the interstitial spaces around the rack modules and within the storage cells must be modeled in an accurate manner. The Coulomb friction coefficient at the pedestal-to-pool liner interface may lie in a rather wide range and a conservative value of friction cannot be prescribed a priori. Finally, the analysis must consider that a rack module may be fully or partially loaded with fuel assemblies or may be entirely empty. The pattern of loading in a partially loaded rack may also have innumerable combinations. In short, there are a large number of parameters with potential influence on the rack motion. A comprehensive structural evaluation must be able to incorporate all of these effects, in a finite number of analyses, without sacrificing conservatism.

The three-dimensional dynamic model of a single spent fuel rack was introduced by Holtec International in 1980 and has been used in many re-rack projects since that time. These re-rack projects include Turkey Point, St. Lucie, and Diablo Canyon. The details of this classical methodology are presented in Reference 10. The three-dimensional model of a typical rack in the spent fuel pool handles the array of variables as follows:

- Interface Coefficient of Friction

  Coefficient of friction (COF) values are assigned at each interface, which reflect the realities of stainless steel-to-stainless steel contact. The mean value of coefficient of friction is 0.5, and the limiting values are based on experimental data, which are bounded by the values 0.2 and 0.8 (Reference 21).

- Impact Phenomena

  Compression-only spring elements, with gap capability, are used to provide for opening and closing of interfaces, such as the pedestal-to-bearing pad interface, the fuel assembly-to-cell wall interface, and the rack-to-rack and rack-to-pool wall potential contact locations.

- Fuel Loading Scenarios

  The dynamic analyses performed for the AP1000 assume that all fuel assemblies within the rack rattle in unison throughout the seismic event, which obviously exaggerates the contribution of impact against the cell wall. An attenuation factor can be used to adjust for the random component of fuel assembly rattling. However, in this analysis, the attenuation factor equals one for all simulations (that is, fuel assemblies conservatively move perfectly in-phase).

- Fluid Coupling

  Holtec International extended Fritz's classical two-body fluid coupling model (Reference 16) to multiple bodies and used it to perform a two-dimensional multi-rack analysis. Subsequently, laboratory experiments were conducted to validate the multi-rack fluid coupling theory. This technology is incorporated in the Whole Pool Multi-Rack (WPMR) analysis, which permits simultaneous simulation of all racks in the pool. In its simplest form, the so-called "fluid coupling effect" (References 11 and 16) can be explained by considering the proximate motion of two bodies under water. If one body (mass m_1) vibrates adjacent to a second body (mass m_2), and both bodies are submerged in frictionless fluid, then Newton's equations of motion for the two bodies are as follows:

  $$(m_1 + M_{11}) A_1 + M_{12} A_2 = \text{applied forces on mass } m_1 + O(X_1^2)$$

  $$M_{21} A_1 + (m_2 + M_{22}) A_2 = \text{applied forces on mass } m_2 + O(X_2^2)$$

  A_1, A_2 denote absolute accelerations of masses m_1 and m_2, respectively, and the notation $O(X^2)$ denotes nonlinear terms. The fluid adds mass to the body (M_{11} to mass m_1), and an inertial force proportional to acceleration of the adjacent body (mass m_2). Thus, acceleration of one body

affects the force field on another. This force field is a function of inter-body gap, reaching large values for small gaps. Lateral motion of a fuel assembly inside a storage location is subject to this effect. The fluid coupling, in general, is always present when a series of closely spaced bodies (fuel racks) undergo transient motion in a submerged spent fuel pool. The fluid coupling effect encompasses interaction between every set of racks in the pool (that is, the motion of one rack produces fluid forces on all other racks and on the pool walls). Both near-field and far-field fluid coupling effects are included in the analysis. During the seismic event, all racks in the pool are subject to the input excitation simultaneously. The motion of each freestanding module is autonomous and independent of others as long as they do not impact each other and no water is present in the pool. As noted in References 11 and 16, the fluid forces can reach rather large values in closely spaced geometries. It is, therefore, essential that the contribution of the fluid forces be included in a comprehensive manner. This is possible only if all racks in the pool are allowed to execute three-dimensional motion in the mathematical model. The fluid coupling effects between all freestanding racks must be included in the model to properly account for the interaction of the hydrodynamic forces with the inertia and friction forces. The WPMR model simulates the three-dimensional motion of all modules simultaneously. The derivation of the fluid coupling matrix relies on the principle of continuity and Kelvin's recirculation theorem. The derivation of the fluid coupling matrix has been verified by an extensive set of shake table experiments (Reference 16).

2.2.2.2 Specific Modeling Details for a Single Rack

The "building block" for the WPMR analysis is a three-dimensional multi-degree of freedom model for each single spent fuel rack. For the WPMR dynamic analysis, each rack, plus contained rattling fuel, is modeled as a 22 Degree of Freedom (DOF) system. The rack cellular structure elasticity is modeled by a three-dimensional beam having 12 DOF (three translation and three rotational DOF at each end so that two-plane bending, tension/compression, and twist of the rack are accommodated). An additional two horizontal DOFs are ascribed to each of five rattling fuel masses, which are located at heights 0H, 0.25H, 0.5H, 0.75H, and H, where H is the height of a storage cell above the baseplate. While the horizontal motion of the rattling fuel mass is associated with five separate masses, the totality of the fuel mass is associated with the vertical motion and it is assumed that there is no fuel rattling in the vertical direction. In other words, the vertical displacement of the fuel is coupled with the vertical displacement of the rack (that is, degree of freedom "P3" in Figure 2-4) by lumping the entire stored fuel mass (in the vertical direction only) with the vertical rack mass at the baseplate level.

The beam model for the rack is assumed supported, at the base level, on four pedestals modeled with non-linear elements; these elements are properly located with respect to the centerline of the rack beam, and allow for arbitrary rocking and sliding motions. The horizontal rattling fuel masses transfer load to the spent fuel rack through compression-only gap spring elements, oriented to allow impacts of each of the five rattling fuel masses with the rack cell in either or both horizontal directions at any instant in time. Figure 2-4 illustrates the typical dynamic rack model with the degrees of freedom shown for both the AP1000 Spent Fuel Storage Racks and for the rattling fuel mass. Table 2-18 defines the nodal DOFs for

the dynamic model of a single rack as depicted in Figure 2-4. In order to simulate this behavior, the stored fuel mass is distributed among the five lumped mass nodes, for all racks, as follows:

	% of total stored fuel mass
• Top of rack (Node 2)	12.5
• 3/4 height (Node 3)	25
• 1/2 height (Node 4)	25
• 1/4 height (Node 5)	25
• Bottom of rack (Node 1)	12.5

(See Figure 2-4.)

The stiffness of pedestal springs that simulate rack pedestal to the floor compression-only contact is modeled using contact and friction elements at the locations of the pedestals between pedestal and floor. Four contact springs (one at each corner location) and eight friction elements (two per pedestal) are included in each 22 DOF rack model.

Also shown in Figure 2-4 is a model detail of a typical support with a vertical compression-only gap element and two orthogonal elements modeling frictional behavior. These friction elements resist lateral loads, at each instant in time, up to a limiting value set by the current value of the normal force times the coefficient of friction. Figures 2-5 through 2-7 show schematic diagrams of the various (linear and non-linear) elements that are used in the dynamic model of a typical spent fuel rack. Specifically, Figure 2-5 shows the location of the compression-only gap elements that are used to simulate the potential for rack-to-rack or rack-to-wall contact at every instant in time. Figure 2-6 shows the four compression-only gap elements at each rattling mass location, which serve to simulate rack-to-fuel assembly impact in any orientation at each instant in time. Figure 2-7 shows a two-dimensional elevation schematic depicting the five fuel masses and their associated gap/impact elements, the typical pedestal friction and gap impact elements. This figure combines many of the features shown in Figures 2-5 and 2-6, and it provides an overall illustration of the dynamic model used for the AP1000 Spent Fuel Storage Racks.

Finally, Figure 2-8 provides a schematic diagram of the coordinates and the beam springs used to simulate the elastic bending behavior and shear deformation of the rack cellular structure in two-plane bending. Not shown are the linear springs modeling the extension, compression, and twisting behavior of the cellular structure.

Mass Matrix

In addition to the structural mass, the following hydrodynamic effects of the pool water are included in the total mass matrix:

- Rack-to-fuel hydrodynamic mass due to fluid motion inside each of the rack cells
- Hydrodynamic mass due to fluid movement around racks in the interstitial spaces between modules
- Hydrodynamic mass effects under the baseplate of each rack

Stiffness Matrix

The spring stiffnesses associated with the elastic elements that model the behavior of the assemblage of cells within a rack are based on the representation developed in Reference 11. Tension-compression behavior and twisting behavior are each modeled by a single spring with linear or angular extension involving the appropriate coordinates at each end of the rack beam model. For simulation of the beam bending stiffness, a model is used consistent with the techniques of the reference based on a bending spring and a shear spring for each plane of bending, which connects the degrees of freedom associated with beam bending at each end of the rack. Impact and friction behavior is included using the piecewise linear formulations similarly taken from the reference.

The AP1000 Spent Fuel Storage Racks are subject to the ASB99 Floor Response Spectra for the AP1000 Spent Fuel Racks provided in Reference 19. Six runs, which are summarized in Table 2-4, are performed to bound possible coefficient of friction values to verify convergence, and to measure the sensitivity to variations in the spring stiffnesses used to model the behavior of the rack.

2.2.3 Simulation and Solution Methodology

The WPMR analysis process is the vehicle available for displacement and load analysis of each rack in the pool, and it also serves to establish the presence or absence of specific rack-to-rack or rack-to-wall impacts during a seismic event. Recognizing that the analytical work effort must deal with stress and displacement criteria, the sequence of model development and analysis steps that are undertaken for each simulation are summarized in the following:

a. Prepare three-dimensional dynamic models of the assemblage of all rack modules in the pool. Include all fluid coupling interactions and mechanical couplings appropriate to performing an accurate non-linear simulation.

b. Perform non-linear WPMR dynamic analyses for the assemblage of racks in the pool. Archive for post-processing appropriate displacement and load outputs from the dynamic model.

c. Perform stress analysis of high stress areas for rack dynamic runs. Demonstrate compliance with American Society for Mechanical Engineers (ASME) Code Section III, subsection NF (Reference 12) limits on stress and displacement. The high stress areas are associated with the pedestal-to-baseplate connection. In addition, some local evaluations are performed for the bounding case to ensure that the fuel remains protected under all impact loads.

For the transient analyses performed in part b, a step-by-step solution in time, which uses a central difference algorithm, is used to obtain a solution. The WPMR simulation model serves as the foundation for the analyses performed herein. The solver computer algorithm, implemented in the Holtec Proprietary Code MR216 (a.k.a. DYNARACK), is given in Reference 11, and the documentation is presented in Reference 13.

Using the 22-DOF structural model for every rack that comprises a WPMR simulation, equations of motion corresponding to each degree-of-freedom are obtained using Lagrange's formulation of the

dynamic equations of motion (Reference 11). The system kinetic energy includes contributions from the structural masses defined by the 22-DOF model.

Results are archived at appropriate time intervals for permanent record and for subsequent post-processing for structural integrity evaluations as follows:

- All generalized nodal displacement coordinate values in order to later determine the motion of the rack
- All load values for linear springs representing beam elasticity
- All load values for compression-only gap springs representing pedestals, rack-to-fuel impact, and rack-to-rack and rack-to-wall impacts
- All load values for friction springs at the pedestal/platform interface

2.2.4 Conservatisms Inherent in Methodology

The following items are built-in conservatisms:

- All fuel rattling mass at each level is assumed to move as a unit thus maximizing impact force and rack response.
- Spring rates are computed in a conservative manner to use maximum values in the analysis. This tends to conservatively overestimate peak impact forces.

2.3 KINEMATIC AND STRESS ACCEPTANCE CRITERIA

2.3.1 Introduction

The AP1000 Spent Fuel Storage Racks are designed as seismic Category I. The U.S. Office of Technology, Position Paper (Reference 5) and the U.S. NRC Standard Review Plan 3.8.4 (Reference 6) state that the ASME Code Section III, subsection NF (Reference 12), as applicable for Class 3 components, is an appropriate vehicle for design. In addition, the stress analysis of the spent fuel racks satisfies all of the applicable provisions in NRC Regulatory Guide 1.124, Revision 1 (Reference 28) for components designed by the linear elastic analysis method. In the following sections, the ASME limits are set down first, followed by any modifications by project specification, where applicable.

2.3.2 Kinematic Criteria

The AP1000 Spent Fuel Storage Racks should not exhibit rotations to cause the rack to overturn (that is, ensure that the rack does not slide off the bearing pads, or exhibit a rotation sufficient to bring the center of mass over the corner pedestal).

2.3.3 Stress Limit Criteria

For thoroughness, the Standard Review Plan load combinations were used. Stress limits must not be exceeded under the required load combinations. The loading combinations shown in Table 2-5 are applicable for freestanding racks that are made of steel. (Note that there is no operating basis earthquake [OBE] event defined for the AP1000; therefore, loading conditions associated with an OBE event are not considered.)

2.3.4 Stress Limits for Various Conditions Per ASME Code

Stress limits for Normal Conditions are derived from the ASME Code, Section III, subsection NF. Parameters and terminology are in accordance with the ASME Code. The AP1000 Spent Fuel Storage Racks are freestanding; thus, there is minimal or no restraint against free thermal expansion at the base of the rack. Moreover, thermal stresses are secondary, which strictly speaking, have no stipulated stress limits in Class 3 structures or components when acting in concert with seismic loadings. Thermal loads applied to the rack are, therefore, not included in the stress combinations involving seismic loadings.

Material properties for analysis and stress evaluation are provided in Table 2-6.

2.3.4.1 Normal Conditions (Level A)

Normal conditions are as follows:

- Tension

  Allowable stress in tension on a net section is:

  $$F_t = 0.6\ S_y$$

  where S_y is the material yield strength at temperature. (F_t is equivalent to primary membrane stress.)

- Shear

  Allowable stress in shear on a net section is:

  $$F_v = 0.4\ S_y$$

- Compression

Allowable stress in compression (F_a) on a net section of Austenitic material is:

$$F_a = S_y(0.47 - kl/444r)$$

where kl/r < 120 for all sections, and

l = unsupported length of component.

k = length coefficient which gives influence of boundary conditions, for example:
k = 1 (simple support both ends)
k = 2 (cantilever beam)
k = 0.5 (clamped at both ends)

Note: Evaluations conservatively use k = 2 for all conditions.

r = radius of gyration of component = c/2.45 for a thin wall box section of mean side width c.

- Bending

Allowable bending stress (F_b) at the outermost fiber of a net section due to flexure about one plane of symmetry is:

$$F_b = 0.60\ S_y$$

- Combined Bending and Compression

Combined bending and compression on a net section satisfies:

$$f_a/F_a + C_{mx}f_{bx}/D_xF_{bx} + C_{my}f_{by}/D_yF_{by} < 1.0$$

where:

f_a	=	Direct compressive stress in the section
f_{bx}	=	Maximum bending stress for bending about x-axis
f_{by}	=	Maximum bending stress for bending about y-axis
C_{mx}	=	0.85
C_{my}	=	0.85
D_x	=	$1 - (f_a/F'_{ex})$
D_y	=	$1 - (f_a/F'_{ey})$
$F'_{ex,ey}$	=	$(\pi^2 E)/(2.15\ (kl/r)_{x,y}^2)$

and subscripts x and y reflect the particular bending plane.

- Combined Flexure and Axial Loads

  Combined flexure and tension/compression on a net section satisfies:

$$(f_a/0.6\ S_y) + (f_{bx}/F_{bx}) + (f_{by}/F_{by}) < 1.0$$

- Welds

  Allowable maximum shear stress (F_w) on the net section of a weld is:

$$F_w = 0.3\ S_u$$

  where S_u is the material ultimate strength at temperature. For the area in contact with the base metal, the shear stress on the gross section is limited to $0.4S_y$.

2.3.4.2 Upset Conditions (Level B)

Although the ASME Code allows an increase in allowables above those appropriate for normal conditions, any evaluations performed herein conservatively use the normal condition allowables.

2.3.4.3 Faulted (Abnormal) Conditions (Level D)

Section F-1334 (ASME Section III, Appendix F [Reference 26]), states that limits for the Level D condition are the smaller of 2 or $1.167S_u/S_y$ times the corresponding limits for the Level A condition if $S_u > 1.2S_y$, or 1.4 if $S_u \leq 1.2S_y$ except for requirements specifically listed below. S_u and S_y are the ultimate strength and yield strength at the specified rack design temperature. Examination of material properties for 304L stainless demonstrates that 1.2 times the yield strength is less than the ultimate strength. Since 1.167 * (66,200/21,300) = 3.1, the multiplier of 2.0 controls.

Exceptions to the above general multiplier are the following:

- Stresses in shear in the base metal shall not exceed the lesser of $0.72S_y$ or $0.42S_u$. In the case of the austenitic stainless material used here, $0.72S_y$ governs.

- Axial compression loads shall be limited to 2/3 of the calculated buckling load.

- Combined Axial Compression and Bending – The equations for Level A conditions shall apply except that:

$$F_a = 0.667 \text{ x Buckling Load/Gross Section Area,}$$

  and $F_{ex,ey}$ may be increased by the factor 1.65.

- For welds, the Level D allowable maximum weld stress is not specified in Appendix F of the ASME Code. An appropriate limit for weld throat is conservatively set here as:

$$F_w = (0.3\ S_u) \times \text{factor}$$

where:

Factor = (Level D shear stress limit)/(Level A shear stress limit)
= $0.72 \times S_y / 0.4 \times S_y = 1.8$

2.3.5 Dimensionless Stress Factors

In accordance with the methodology of the ASME Code, Section NF, where both individual and combined stresses must remain below certain values, the stress results are presented in dimensionless form. Dimensionless stress factors are defined as the ratio of the actual developed stress to the specified limiting value. The limiting value of each stress factor is 1.0 based on an evaluation that uses the allowable strength appropriate to Level A or Level D loading as discussed above.

R_1 = Ratio of direct tensile or compressive stress on a net section to its allowable value (note pedestals only resist compression)

R_2 = Ratio of gross shear on a net section in the x-direction to its allowable value

R_3 = Ratio of maximum bending stress due to bending about the x-axis to its allowable value for the section

R_4 = Ratio of maximum bending stress due to bending about the y-axis to its allowable value for the section

R_5 = Combined flexure and compression factor (as defined in subsection 2.3.4.1)

R_6 = Combined flexure and tension (or compression) factor (as defined in subsection 2.3.4.1)

R_7 = Ratio of gross shear on a net section in the y-direction to its allowable value

At any location where stress factors are reported, the actual stress at that location may be recovered by multiplying the reported stress factor R by the allowable stress for that quantity. For example, if a reported Level A combined tension and two plane bending stress factor is $R_6 = 0.85$, and the allowable strength value is $0.6S_y$, then the actual combined stress at that location is Stress = $R_6 \times (0.6S_y) = 0.51S_y$.

2.4 ASSUMPTIONS

The following assumptions are used in the analysis:

- Fluid damping is neglected. This is a conservative assumption.
- The total effect of *n* individual fuel assemblies rattling inside the storage cells in a horizontal plane is modeled as one lumped mass at each of five levels in the fuel rack. Thus, the effects of chaotic fuel mass movement are conservatively ignored.
- Fluid coupling forces are calculated based on the nominal fluid gaps. The fluid gaps are not updated according to the rack displacements.

2.5 INPUT DATA

2.5.1 Rack Data

Table 2-7 contains information regarding the AP1000 Spent Fuel Storage Racks and fuel data that are used in the analysis. Information is taken from the Holtec rack drawings (Reference 9) (unless noted otherwise).

2.5.2 Structural Damping

Associated with every stiffness element is a damping element with a coefficient consistent with 4% of critical linear viscous damping. This is consistent with the ASB99 Design-Basis Floor Response Spectra set for the AP1000 Spent Fuel Storage Racks provided in Reference 19 and the Westinghouse AP1000 Seismic Design Criteria provided in Reference 22.

2.5.3 Material Data

The necessary material data are shown in Table 2-6. This information is taken from ASME Code Section II, Part D (Reference 14). The values listed correspond to a temperature of 200°F.

2.6 COMPUTER CODES

Computer codes used in this analysis are presented in Table 2-8.

2.7 ANALYSES

2.7.1 Acceptance Criteria

The dimensionless stress factors, discussed in subsection 2.3.5, must be less than 1.0. In addition:

- Cell wall stress shall be shown to remain below the critical buckling stress.
- Welds and local stresses must remain below the allowable stress limits corresponding to the material and load conditions, as discussed in greater detail in following sections.

2.7.2 Dynamic Simulations

As discussed earlier, two simulations are performed. The simulations consider the ASB99, Floor Response Spectra and are required to satisfy the stress and kinematic criteria of Reference 5 and Reference 6.

2.8 RESULTS OF ANALYSES

The following subsections contain the results obtained from the post-processor DYNAPOST (Reference 15) for the AP1000 Spent Fuel Storage Racks under the ASB99, Floor Response Spectra. With eight racks in each model, there are nine tables per simulation; the first one details the rack input information and provides an overall summary of the analysis, while the other eight tables provide a complete listing of results for each AP1000 Spent Fuel Storage Rack.

2.8.1 Time History Simulation Results

Table 2-9 presents the results for major parameters of interest for the AP1000 Spent Fuel Storage Racks for each simulation. Run numbers are as listed in Table 2-4.

2.8.1.1 Rack Displacements

The post-processor results summarized in Table 2-10 provide the maximum absolute displacements at the top and bottom corners (in the east-west or north-south horizontal direction) relative to the pool slab.

2.8.1.2 Pedestal Vertical Forces

Run number 5 provides the maximum vertical load on any pedestal. This may be used to assess the structural integrity of the pool slab under the seismic event.

2.8.1.3 Pedestal Friction Forces

Run number 3 provides the maximum shear loads; the value is used as an input loading to evaluate the female pedestal-to-baseplate weld.

2.8.1.4 Impact Loads

The impact loads – such as fuel-to-cell wall, rack-to-rack, and rack-to-wall impacts – are discussed below.

Fuel-to-Cell Wall Impact Loads

The maximum fuel-to-cell wall impact load, at any level in the rack, occurs during run number 6.

For the five-lumped mass model (with 25% at the 1/4 points and 12.5% at the ends), the maximum g-load that the rack imparts on the fuel assembly can be computed as:

$$a = \frac{4F}{w} = 2.66 \cdot g$$

where:

a = maximum lateral acceleration in g's
F = maximum fuel-to-cell wall impact force (= 1,149 lbf)
w = weight of one fuel assembly (conservatively taken to be 1,730 lbs)

Rack-to-Rack and Rack-to-Wall Impacts

The solver summary result files from Reference 13 in all of the simulations were manually scanned to determine the maximum impact on each side of the rack. No rack-to-wall impacts occur at any time instant during any simulation. Rack-to-rack impacts do occur at the top of rack elevation between adjacent Region 2 racks and also at the baseplate elevation of all racks. The maximum rack-to-rack impact loads at the baseplate elevation and top of rack elevation are 42,950 lb and 72,080 lb, respectively, during the postulated safe shutdown earthquake (SSE) event. These impact loads do not result in damage to the racks that would prevent fuel retrievability.

2.8.2 Rack Structural Evaluation

2.8.2.1 Rack Stress Factors

With time-history results available for pedestal normal and lateral interface forces, the limiting bending moment and shear force at the baseplate-to-pedestal interface may be computed as a function of time. In particular, maximum values for the previously defined stress factors can be determined for every pedestal in the AP1000 Spent Fuel Storage Racks. The maximum stress factor for the AP1000 Spent Fuel Storage Racks from each simulation is reported in the result tables and Table 2-9. Using this information, the structural integrity of the pedestal can be assessed. The net section maximum (in time) bending moments and shear forces can also be determined at the bottom of the cellular structure. Based on these, the maximum stress in the limiting rack cell (box) can be evaluated.

The summary of the maximum stress factors for the AP1000 Spent Fuel Storage Racks, for each of the simulations detailed in Table 2-4, is provided in Table 2-11. The tables also report the stress factors for the AP1000 Spent Fuel Storage Racks cellular cross section just above the baseplate. These locations are the most heavily loaded net sections in the structure so that satisfaction of the stress factor criteria at these locations ensures that the overall structural criteria set forth in subsection 2.3.3 are met.

An adjustment factor accounting for the ASME Code slenderness ratio has been calculated. The adjustment factors are identified with * in the Table 2-11.

All stress factors, as defined in Section 2.3, are less than the mandated limit of 1.0 for all racks for the governing faulted condition examined. Therefore, the rack is able to maintain its structural integrity under the worst loading conditions.

2.8.2.2 Weld Stresses

Weld locations in the AP1000 Spent Fuel Storage Racks subjected to significant seismic loading are at the bottom of the rack at the baseplate-to-cell connection, at the top of the pedestal support at the baseplate connection, and at the cell-to-cell connections. Bounding values of resultant loads are used to qualify the connections.

a. Baseplate-to-Rack Cell Welds

Reference 12 (ASME Code Section III, subsection NF) permits, for Level A or B conditions, an allowable weld stress $\tau = .3\ S_u$. Conservatively assuming that the weld strength is the same as the lower base metal ultimate strength, the allowable stress is given by $\tau = .3 * (66{,}200) = 19{,}518$ psi. As stated in subsection 2.3.4.3, the allowable for Level D is $0.54\ S_u$, giving an allowable of 35,748 psi.

Weld stresses are determined through the use of a simple conversion (ratio) factor (based on area ratios) applied to the corresponding stress factor in the adjacent rack material. This conversion factor is developed from the differences in base material thickness and length versus weld throat dimension and length:

$$\frac{0.075*(8.8+0.075)}{0.0625*0.7071*7.0} = 2.1516$$

where:

0.075	=	the cell wall thickness
8.8 + 0.075	=	the mean box dimension
0.0625*0.7071	=	the box-baseplate fillet weld throat size
7.0	=	the length of the weld

The highest predicted cell-to-baseplate weld stress is calculated based on the highest R6 value for the rack cell region tension stress factor and R2 and R7 values for the rack cell region shear stress factors (see subsection 2.3.5 for definition of these factors). These cell wall stress factors are converted into weld stress values as follows:

- For ASB99 Simulation

$$\{[R6 * (1.2)]^2 + [R2 * (0.72)]^2 + [R7 * (0.72)]^2\}^{1/2} * S_y * \text{Ratio} =$$

$$\{[0.441 * (1.2)]^2 + [0.069 * (0.72)]^2 + [0.082 * (0.72)]^{21/2} * (21{,}300) * 2.1516 = 25{,}047 \text{ psi}$$

The above calculations are conservative because the maximum stress factors used above do not all occur at the same time instant.

Table 2-12 shows that the weld stresses are acceptable and have safety factors greater than 1.

The corresponding maximum base metal shear stress is shown in Table 2-13.

b. Baseplate-to-Pedestal Welds

The finite element code ANSYS is used to resolve tension and compression stresses in the baseplate-to-pedestal weld due to the combined effects of a vertical compressive load in the pedestal and a bending moment caused by pedestal friction. The compression interface between the baseplate and the pedestal is modeled using contact elements. The perimeter nodes on the pedestal are connected to the baseplate by spring elements in order to simulate tension in the weld. The maximum instantaneous friction force on a single pedestal from the rack seismic analysis is conservatively applied to the finite element model in the horizontal x- and y-directions simultaneously, along with the concurrent vertical load, at the appropriate offset location. The perimeter nodes on the pedestal are restrained to move only in the vertical direction so that the spring elements only resist bending. The limiting ANSYS results are combined with the maximum horizontal shear loads to obtain the maximum weld stress, which occurs at the corner of the pedestal where the tensile stress in the weld due to bending is at its maximum. Table 2-14 summarizes the result.

c. Cell-to-Cell Welds

Cell-to-cell connections are by a series of connecting welds along the cell height. Stresses in storage cell-to-cell welds develop due to fuel assembly impacts with the cell wall. These weld stresses are conservatively calculated by assuming that fuel assemblies in adjacent cells are moving out of phase with one another so that impact loads in two adjacent cells are in opposite directions; this tends to separate the two cells from each other at the weld. Cell-to-cell weld calculations are based on the maximum stress factor from all runs. Both the weld and the base metal shear results are reported in Tables 2-16 and 2-17, respectively.

2.8.2.3 Pedestal Thread Shear Stress

Table 2-15 provides the limiting thread stresses under faulted conditions. The maximum average shear stress in the engagement region is 16,617 psi, which occurs during run number 5. This computed stress is applicable to both the male and female pedestal threads.

The allowable shear stress for Level D conditions is the lesser of: $0.72\ S_y = 18{,}000$ psi or $0.42\ S_u = 29{,}400$ psi (based on S_y and S_u for SA240-304 at 200°F). Therefore, the former criterion controls and the limiting result are detailed in Table 2-15.

2.8.3 Dead Load Evaluation

The dead load condition is not a governing condition for spent fuel racks since the general level of loading is far less than the SSE load condition. The maximum pedestal load is low, and further stress evaluations are unnecessary.

Description	Level A Maximum Pedestal Load (lbf)
Dry Weight of 12x11 Rack	21,730
Dry Weight of 132 Intact Fuel Assemblies	228,360
Total Dry Weight	250,090
Load per Pedestal	62,523

This load will induce low stress levels in the neighborhood of the pedestal, compared with the load levels that exist under the SSE load condition (that is, on the order of 334,000 lb for this rack). Therefore, there are no primary shear loads on the pedestal and since the Level A loads are approximately 20% of the Level D loads, while the Level A limits exceed 50% of the Level D limits, the SSE load condition bounds the dead load condition and no further evaluation is performed for dead load only.

2.8.4 Local Stress Considerations

This subsection presents evaluations for the possibility of cell wall buckling and the secondary stresses produced by temperature effects.

2.8.4.1 Cell Wall Buckling Evaluation

The allowable local buckling stresses in the fuel cell walls (from vertical loading) are obtained by using classical plate buckling analysis on the lower portion of the cell walls. The following formula for the critical stress has been used:

$$\sigma_{cr} = \frac{\beta \times \pi^2 \times E \times t^2}{12 \times b^2 (1 - \nu^2)}$$

Where E = 27.6 x 10^6 psi, ν is Poisson's ratio = 0.3, t = 0.075", b = 8.8". The β factor varies depending on the plate length/width ratio and the boundary support conditions at the sides of the plate. At the base of the rack, the cell wall acts alone in compression for a length of about 6 inches up to the point where the poison sheathing is attached. Above this level, the sheathing provides additional strength against buckling, which is not considered here. Therefore, the length/width ratio for the 8.8-inch wide cell wall is 0.68. For the case of simply supported on two sides perpendicular to the direction of compression with the remaining two sides fixed, the β value is given by Table 9-5 of Reference 25 to be 7.01.

For the given data:

$\sigma_{cr} < 12{,}702$ psi

It should be noted that this calculation is based on the applied vertical stress being uniform along the entire length of the cell wall. In the actual fuel rack, the compressive vertical stress comes from consideration of overall bending of the rack structures during a seismic event and as such is negligible at the rack top and maximum at the rack bottom. It is conservative to apply the above equation to the rack cell wall if σ_{cr} is compared with the maximum compressive stress anywhere in the cell wall. This local

buckling stress limit is not violated anywhere in the body of the rack modules since the maximum compressive stress in the outermost cell is σ = (1.2)(21,300) * R6 (which is 0.441) = 11,272 psi, which is less than 12,702 psi. Therefore, rack cell wall buckling is not a concern.

2.8.4.2 Thermal Stress Evaluation of Isolated Hot Cell

The temperature gradients across the rack structure caused by differential heating effects between one or more filled cells and one or more adjacent empty cells are considered. The worst thermal stress field in a fuel rack is obtained when an isolated storage location has a fuel assembly generating heat at maximum postulated rate and the surrounding storage locations contain no fuel. This secondary stress condition is evaluated alone and not combined with primary stresses from other load conditions.

A thermal gradient between cells will develop when an isolated storage location contains a fuel assembly emitting maximum postulated heat, while the surrounding locations are empty. A conservative estimate of the weld stresses along the length of an isolated hot cell is obtained by considering a beam strip uniformly heated by 50°F, and restrained from growth along one long edge. The 50°F temperature rise envelops the difference between the maximum local spent fuel pool water temperature (174°F) inside a storage cell and the bulk pool temperature (140°F) based on the thermal-hydraulic analysis of the spent fuel pool. The cell wall configuration considered here is shown in figure below.

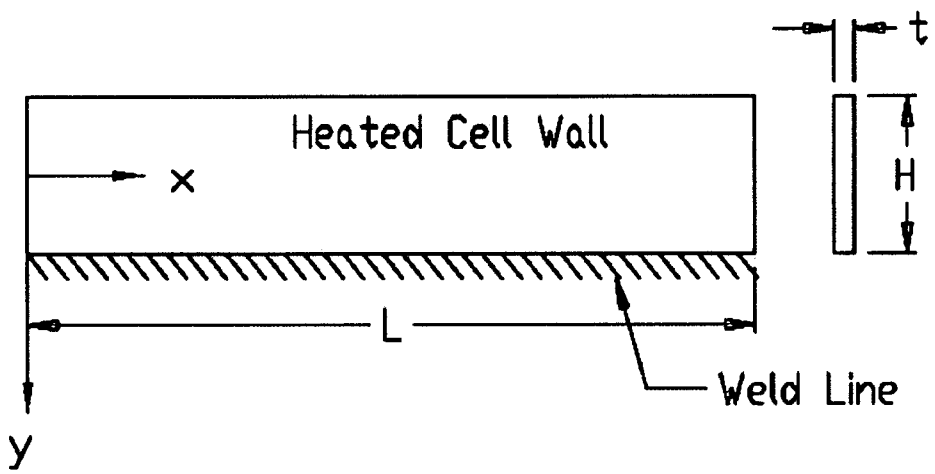

The strip is subjected to the following boundary conditions:

- Displacement U_x (x,y) = 0 at x = 0 and at y = H/2 for all x
- Average force N_x (x) = 0 at x = L

Using shear beam theory and subjecting the strip to a uniform temperature rise ΔT = 50°F, we can calculate an estimate of the maximum value of the average shear stress in the strip. The final shear stress result for the strip is found to be

$$\tau_{max} = \frac{E \alpha \Delta T}{0.931} \qquad \text{(maximum at x = L)}$$

where $E = 27.6 \times 10^6$ psi, $\alpha = 9.5 \times 10^{-6}$ in/in °F and $\Delta T = 50°F$.

Therefore, we obtain an estimate of maximum weld shear stress in an isolated hot cell, due to thermal gradient, as

$$\tau_{max} = 14{,}082 \text{ psi}$$

Since this is a secondary thermal stress, the allowable shear stress criteria for faulted conditions ($0.42*S_u$=27,804 psi) is used to indicate that this maximum shear is acceptable. Therefore, there is a safety factor = 27,804 / 14,082 = 1.97 against cell wall shear failure due to secondary thermal stresses from cell wall growth under the worst case hot cell conditions.

2.8.5 Hypothetical Fuel Assembly Drop Accidents

Three fuel assembly drop accident analyses were performed for Region 1 and Region 2 spent fuel racks respectively: 1) a drop of a spent fuel assembly with control elements plus a lifting tool (conservatively modeled as a total weight of 3,100 lb) from 36 inches above the top of the AP1000 Spent Fuel Rack with subsequent impact on the edge of a cell; 2) a drop of a spent fuel assembly with control elements plus a lifting tool from 36 inches above the top of the rack down through an empty cell with impact on the rack baseplate away from the rack pedestal; and 3) a drop of a spent fuel assembly with control elements plus a lifting tool from 36 inches above the top of the rack down through an empty cell with impact on the rack baseplate directly above the rack pedestal. The objective of the analyses was to assess the extent of permanent damage to the rack and to evaluate the structural integrity of the spent fuel pool liner.

All analyses were performed using the dynamic simulation code LS-DYNA (Reference 24). The impact velocity between the dropped fuel and the rack was calculated by considering the resistance of the spent fuel pool water including the confinement effect of the rack cell. A finite element model of one-quarter of the spent fuel rack plus a single fuel assembly was modeled using appropriate shell and solid body elements available in LS-DYNA. The fuel assembly model, which is shown in Figure 2-9, consists of four parts: a rigid bottom end fitting, an elastic beam representing the fuel rods, a lumped mass at the top end of the beam representing the handling tool, and a thin rigid shell that defines the enveloping size and shape of the fuel assembly. The mass and cross-sectional area properties of the elastic beam are based on the entire array of fuel rods (cladding material only). The fuel mass is lumped with the bottom end fitting. Appropriate non-linear material properties have been assigned to the rack components to permit yielding and permanent deformation to occur. Figures 2-10 and 2-11 show the details of the finite element model of the Region 1 spent fuel rack and Region 2 spent fuel rack, respectively.

For the drop to the top of the AP1000 Spent Fuel Rack, the fuel assembly is assumed to strike the edge of an exterior cell at a speed corresponding to a 36-inch drop and to remain vertical as it is brought to a stop by the resisting members of the rack. The objective is to demonstrate that the extent of permanent damage to the impacted rack does not extend to the beginning of the active fuel region. For the AP1000 fuel, the active fuel region begins approximately 21.1 inches below the top of either the Region 1 or Region 2 rack.

For the drop through an empty cell to the baseplate, two extreme drop scenarios were considered in the analysis. The first scenario considered the maximum deformation of the rack baseplate by assuming that

the impact occurs near the center of the rack. As the baseplate of the rack is connected to the cells by welding, a portion of the welding is expected to fail under this drop scenario. The energy from the falling fuel assembly is absorbed by weld failure plus deformation of the baseplate toward the floor. The fuel assemblies surrounding the impacted cell follows the baseplate deformation, and the objective is to determine how many fuel assemblies displace an amount sufficient to bring their active fuel region below the limit of the absorbing material attached to each fuel cell wall. In the case of the AP1000 Spent Fuel Racks, a 2-inch vertical movement of a fuel assembly, relative to the cell wall, will not require any new criticality evaluation. For the drop scenario where the impact occurs inside the empty cell directly above a rack pedestal, the spent fuel pool floor is assumed to be constructed using 4,000 psi concrete and the thickness of the spent fuel floor stainless steel liner is assumed to be 3/16 inch thick. The objective of this impact analysis was to assess the damage in the rack pedestal and in the spent fuel pool liner.

The results from the analyses are shown in Figures 2-12, 2-13, and 2-14:

- For the drop to the top of the rack, the bounding damage occurs in the Region 2 rack with the extent of permanent damage limited to a depth of 14.06 inches as shown in Figure 2-12. Therefore, the active fuel region remains surrounded by an undamaged cell wall and no further evaluation is required.

- For the drop to the baseplate of the rack, the maximum baseplate deformation occurs in the Region 2 rack. Figure 2-13 shows that nine fuel assemblies (including the dropped assembly) are moved downward more than 2 inches and expose active fuel on all four sides. An additional 12 fuel assemblies may drop a sufficient distance to expose active fuel on 2 sides. This scenario is addressed in subsection 2.4.9 of Reference 4.

- For the drop over a rack pedestal, the plastic strain in the spent fuel pool liner is shown in Figure 2-14. Since the liner strain remains elastic, the postulated drop event will not breach the spent fuel pool liner.

2.8.6 Stuck Fuel Assembly Evaluation

A nearly empty rack with one corner cell occupied is subject to an upward load of 2,000 lbf, which is assumed to be caused by the fuel sticking while being removed. The ramification of the loading is two-fold:

1. The upward load creates a force and a moment at the base of the rack;
2. The loading induces a local tension in the cell wall and shear stresses in the adjacent welds.

Strength of materials calculations have been performed to determine the maximum stress in the rack cell structure due to a postulated stuck fuel assembly. The results are summarized in Table 2-19.

2.9 CONCLUSIONS

From the results of the WPMR analyses, the following conclusions are made regarding the design and layout of the AP1000 Spent Fuel Storage Racks:

- All rack cell wall and pedestal stress factors are below the allowable stress factor limit of 1.0.
- All weld stresses are below the allowable limits.
- A stuck fuel assembly does not cause a bounding stress condition.
- Fuel assembly drops were analyzed for each rack type.

It is therefore considered demonstrated that the design of the AP1000 Spent Fuel Storage Racks meets the requirements for structural integrity for the postulated Level A and Level D conditions defined.

Per DCD subsection 3.7.5.2, Combined License applicants will prepare site-specific procedures for activities following an earthquake. An activity will be to address measurement of the post-seismic event gaps between spent fuel racks and to take appropriate corrective actions.

Table 2-1 Region 1 Storage Racks	
(All dimensions are in inches; tolerances are not shown because they are Westinghouse Proprietary Information.)	
Parameter	**Value**
Storage Cell Center-to-Center Pitch	10.9
Storage Cell Inner Dimension (Width)	8.8
Inter-Cell Flux Trap Gap	1.644
Storage Cell Length Region 1 Spent Fuel Storage Rack	199.5
Storage Cell Wall Thickness	0.075
Neutron Absorber Material	Metamic
Neutron Absorber Length	172
Neutron Absorber Width	7.5
Neutron Absorber Thickness	0.106
Distance from Top of Rack Baseplate to Bottom of Neutron Absorber	6.23
Neutron Absorber B_4C Loading	31 weight-percent
Neutron Absorber Sheathing Thickness Internal Walls Periphery Walls	 0.035 0.075
Baseplate Thickness	0.75
Baseplate Flow Hole Diameter	6
Rack Pedestal Type (fixed or adjustable)	Adjustable
Rack Pedestal Height (female + male)	2.75
Rack Female Pedestal Dimensions	20 x 20 x 2.25
Rack Male Pedestal Diameter	4.5
Rack Bearing Pad Thickness	1.5

Table 2-2 Region 2 Spent Fuel Pool Storage Racks	
(All dimensions are in inches; tolerances are not shown because they are Westinghouse Proprietary Information.)	
Parameter	**Value**
Storage Cell Center-to-Center Pitch	9.028
Storage Cell Inner Dimension (Width)	8.8
Inter-Cell Flux Trap Gap	N/A
Storage Cell Length	199.5
Storage Cell Wall Thickness	0.075
Neutron Absorber Material	Metamic
Neutron Absorber Length	172
Neutron Absorber Width	7.5
Neutron Absorber Thickness	0.106
Distance from Top of Rack Baseplate to Bottom of Neutron Absorber	6.23
Neutron Absorber B_4C Loading	31 weight-percent
Neutron Absorber Sheathing Thickness Internal Walls Periphery Walls	 0.035 0.075
Baseplate Thickness	0.75
Baseplate Flow Hole Diameter	6
Rack Pedestal Type (fixed or adjustable)	Adjustable
Rack Pedestal Height (female + male)	2.75
Rack Female Pedestal Dimensions	18 x 18x 2.25
Rack Male Pedestal Diameter	4.5
Rack Bearing Pad Thickness	1.5

Table 2-3 Spent Fuel Pool Damaged Fuel Assembly Storage Cells	
(All dimensions are in inches; tolerances are not shown because they are Westinghouse Proprietary Information.)	
Parameter	**Value**
Storage Cell Center-to-Center Pitch	12.35
Storage Cell Inner Dimension (Width)	10.25
Inter-Cell Flux Trap Gap Between Defective Fuel Cells Defective Fuel Cells to Region 2 Cells	 0.91 1.644
Storage Cell Length	199.5
Storage Cell Wall Thickness	0.075
Neutron Absorber Material	Metamic
Neutron Absorber Length	172
Neutron Absorber Width	7.5
Neutron Absorber Thickness	0.106
Distance from Top of Rack Baseplate to Bottom of Neutron Absorber	6.23
Neutron Absorber B_4C Loading	31 weight-percent
Neutron Absorber Sheathing Thickness Internal Walls Periphery Walls	 0.035 0.075

Table 2-4 Simulation Listing

Run Number	Coefficient of Friction	Loading Configuration	Seismic Input (Floor Response Spectra)	Integration Time Step (sec)	Percentage of Calculated Stiffnesses
1	0.2	Fully Loaded	ASB99	1×10^{-5}	100%
2	0.5	Fully Loaded	ASB99	1×10^{-5}	100%
3	0.8	Fully Loaded	ASB99	1×10^{-5}	100%
4	0.8	Fully Loaded	ASB99	1×10^{-5}	80%
5	0.8	Fully Loaded	ASB99	1×10^{-5}	120%
6	0.8	Fully Loaded	ASB99	5×10^{-6}	100%

Table 2-5 Loading Combinations for AP1000 Spent Fuel Storage Racks

Loading Combination	Service Level
$D + L$ $D + L + T_o$	Level A
$D + L + T_a$ $D + L + T_o + P_f$	Level B
$D + L + T_a + E'$	Level D
$D + L + F_d$	The functional capability of the fuel racks should be demonstrated.

Notes:

1. There is no operating basis earthquake (OBE) for the AP1000 plant.
2. The fuel racks are freestanding; thus, there is minimal or no restraint against free thermal expansion at the base of the rack. As a result, thermal loads applied to the rack (T_o and T_a) produce only local (secondary) stresses.

Abbreviations are those used in Reference 6:

D = Dead weight induced loads (including fuel assembly weight)

L = Live load (not applicable to fuel racks since there are no moving objects in the rack load path)

F_d = Force caused by the accidental drop of the heaviest load from the maximum possible height

P_f = Upward force on the racks caused by postulated stuck fuel assembly

E' = Safe Shutdown Earthquake (SSE)

T_o = Differential temperature induced loads based on the most critical transient or steady state condition under normal operation or shutdown conditions

T_a = Differential temperature induced loads based on the postulated abnormal design conditions

Table 2-6 Material Data (ASME – Section II, Part D)

Material	Young's Modulus* E (psi)	Yield Strength S_y (psi)	Ultimate Strength S_u (psi)
Rack Material Data (304L SS @ 200°F)			
SA240-304L	27.6×10^6	21,300	66,200
Support Material Data (200°F)			
SA-240, Type 304L (Upper part of support feet)	27.6×10^6	21,300	66,200
SA-564, Type 630 (Hardened at 1100° F)	28.5×10^6	106,300	140,000

Note:

The table includes material strength data for SA240-304L. Per Reference 9, the spent fuel racks are fabricated from SA240-304, which has higher yield and ultimate strength values than SA240-304L. Unless otherwise noted, safety factors are calculated using the lesser properties of SA240-304L, as provided in the table, for conservatism.

Table 2-7 AP1000 Spent Fuel Storage Racks and Fuel Data

Geometric Parameter		Dimension (in) Unless Noted
Composite Box Data		
Box ID		8.8
Pitch		10.9 (Region 1) 9.028 (Region 2)
Wall Thickness		0.075
Rack Module Data		
Cell Length		199.5 (Region 1) 199.5 (Region 2)
Support Height		2.75
Female Pedestal Side Dimension		20.0 x 20.0 square (Region 1) 18.0 x 18.0 (Region 2)
Female Pedestal Height		2.25
Male Pedestal Diameter		4.5
Total Height		203.0
Baseplate Thickness		0.75
Baseplate Extension		7/8 (Region 1) 1/2 (Region 2)
Fuel Data		
Dry Fuel Wt (lb)		1,730 (Reference 19)
Assembly Size		8.404 (Reference 19)
Rack Details		
Rack	**Array Size**	**Weight (lb)**
A1, A2, A3	9 x 9	25,000
B1, B2, B3, B4	12 x 11	21,730
C1	12 x 10	22,234

Table 2-8 Computer Codes Used for AP1000 Spent Fuel Storage Racks Structural/Seismic Analysis

Code	Version	Description
GENEQ	1.3	Generates artificial time histories from input response spectra set.
CORRE	1.3	Uses results from GENEQ and demonstrates required statistical independence of time histories.
PSD1	1.0	Uses results from GENEQ and compares regenerated Power Spectral Densities with target.
WORKING MODEL	2004	Is a Rigid Body Dynamics code used to improve baseline correction.
VMCHANGE	4.0	For a dry pool, develops a zero matrix of size = (number of racks x 22 DOF per rack).
MULTI	1.55	Incorporates appropriate non-zero values due to structural effects that are put in appropriate locations in the output matrix from VMCHANGE to form the final mass matrix for the analysis. The appropriate non-zero right-hand sides are also developed.
MASSINV	2.1	Calculates the inverse of the mass matrix.
MSREFINE	2.1	Refines the inverse of the mass matrix.
PREDYNA1	1.5	Generates various input lines for the input file required to run the dynamic solver.
PD16	2.1	Generates rack-to-fuel compression-only impact springs, rack-to-ground impact springs, and rack elastic deflection springs for each rack being analyzed and creates the appropriate lines of input for the solver.
SPG16	3.0	Generates compression-only rack-to-rack impact springs for the specific rack configuration in the pool for the solver.
MR216	2.0	Is a solver for the dynamic analysis of the racks; uses an input file from the cumulative output from PREDYNA, PD16, and SPG16, together with the mass matrix, right-hand side matrix, and the final time histories from GENEQ.
DYNAPOST	2.0	Post-Processor for MR216; generates safety factors, maximum pedestal forces, and maximum rack movements.
ANSYS	9.0	Is a general purpose commercial FEA code.
LS-DYNA	970	General purpose commercial FEA code optimized for shock and impact analyses

Table 2-9 Results Summary

Run No.	Coefficient of Friction	Max. Stress Factor	Max. Vertical Load (lbf)	Max. Shear Load (lbf) (X or Y)	Max. Fuel-to-Cell Wall Impact (lbf)
1	0.2	0.343	258,000	48,400	1,080
2	0.5	0.428	311,000	134,000	989
3	0.8	0.426	311,000	194,000	1,125
4	0.8	0.441	325,000	175,000	955
5	0.8	0.440	334,000	165,000	1,130
6	0.8	0.426	311,000	184,000	1,149

Table 2-10 Time History Post-Processor Results

Location on Rack	Maximum Rack Displacement Relative to Floor (in)	Run Number
Base Plate	0.354	1
Top of Rack	1.486	3

Table 2-11 Maximum Stress Factors

Run Number	Pedestal Stress Factor	Cell Wall Stress Factor
1	0.056	$\overset{0.343}{\left(0.343 \times \frac{1}{0.652}\right)} = 0.526$ *
2	0.074	$\overset{0.428}{\left(0.428 \times \frac{1}{0.593}\right)} = 0.722$ *
3	0.082	$\overset{0.426}{\left(0.426 \times \frac{1}{0.593}\right)} = 0.718$ *
4	0.076	$\overset{0.441}{\left(0.441 \times \frac{1}{0.593}\right)} = 0.744$ *
5	0.098	$\overset{0.440}{\left(0.440 \times \frac{1}{0.593}\right)} = 0.742$ *
6	0.086	$\overset{0.426}{\left(0.426 \times \frac{1}{0.593}\right)} = 0.718$ *

Note:
* Adjustment factor accounting for ASME Code Slenderness Ratio

Table 2-12 Baseplate-to-Cell Maximum Weld Stress

Weld Stress (psi)	Allowable Stress (psi)	Safety Factor
24,509	35,748	1.46

Table 2-13 Base Metal Shear Stress at Baseplate-to-Cell Weld Location

Base Metal Shear Stress (psi)	Allowable Stress (psi)	Safety Factor
17,330	18,000*	1.04

Note:
* Based on yield strength of SA240-304 at 200°F (0.72 x 25,000 psi = 18,000 psi).

Table 2-14 Baseplate-to-Pedestal Welds

Weld Stress (psi)	Run No.	Allowable Stress (psi)	Safety Factor
10,820	3	35,748	3.31

Table 2-15 Pedestal Thread Shear Stress

Base Metal Shear Stress (psi)	Allowable Stress (psi)	Safety Factor
16,617	18,000*	1.08

Note:
* Based on yield strength of SA240-304 at 200°F (0.72 x 25,000 psi = 18,000 psi).

Table 2-16 Maximum Cell-to-Cell Weld Stress

Weld Stress (psi)	Allowable Stress (psi)	Safety Factor
11,181	35,748	3.20

Table 2-17 Maximum Base Metal Shear Stress at Cell-to-Cell Weld Location

Base Metal Shear Stress (psi)	Allowable Stress (psi)	Safety Factor
7,906	18,000*	2.28

Note:
* Based on yield strength of SA240-304 at 200°F (0.72 x 25,000 psi = 18,000 psi).

Table 2-18 Degrees of Freedom for Single Rack Dynamic Model

Location (Node)	Displacement			Rotation		
	U_x	U_y	U_z	θ_x	θ_y	θ_z
1	p_1	p_2	p_3	q_4	q_5	q_6
2	p_7	p_8	p_9	q_{10}	q_{11}	q_{12}
Node 1 is assumed to be attached to the rack at the bottom most point. Node 2 is assumed to be attached to the rack at the top most point. Refer to Figure 2-2 for node identification.						
2*	p_{13}	p_{14}				
3*	p_{15}	p_{16}				
4*	p_{17}	p_{18}				
5*	p_{19}	p_{20}				
1*	p_{21}	p_{22}				

where the relative displacement variables q_i are defined as:

$p_i = q_i(t) + U_x(t) i = 1,7,13,15,17,19,21$
$= q_i(t) + U_y(t) i = 2,8,14,16,18,20,22$
$= q_i(t) + U_z(t) i = 3,9$
$= q_i(t) i = 4,5,6,10,11,12$

p_i denotes absolute displacement (or rotation) with respect to inertial space
q_i denotes relative displacement (or rotation) with respect to the floor slab

* denotes fuel mass nodes
U(t) are the three known earthquake displacements

Table 2-19 Results from Stuck Fuel Assembly Evaluation

Item	Calculated Stress (psi)	Allowable Stress (psi)	Safety Factor
Tensile Stress in Cell Wall	2,736	12,780*	4.67
Shear Stress in Cell-to-Cell Weld	3,771	19,860	5.26

Note:

* Conservatively based on Level A limit for tensile stress (0.6 Sy). Stuck fuel assembly load is defined as Service Level B per Table 2-5.

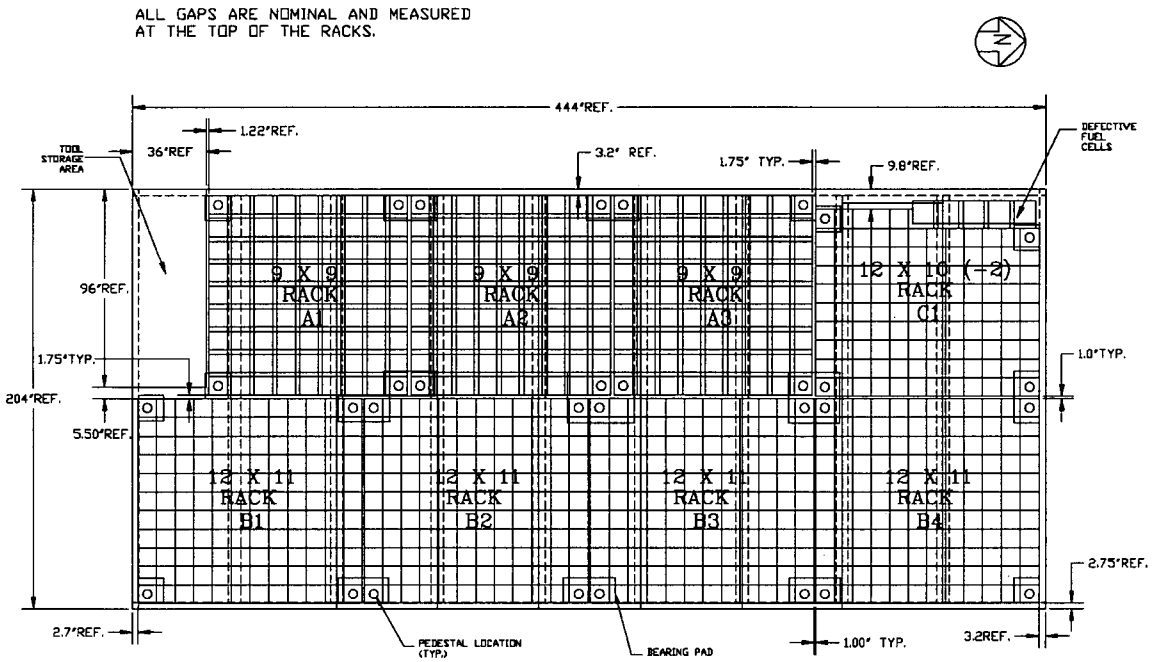

DISCRETE ZONE TWO REGION SPENT FUEL POOL RACK LAYOUT

Figure 2-1 Spent Fuel Pool Storage Layout (889 Total Storage Locations) – Leak Chases Show in Phantom

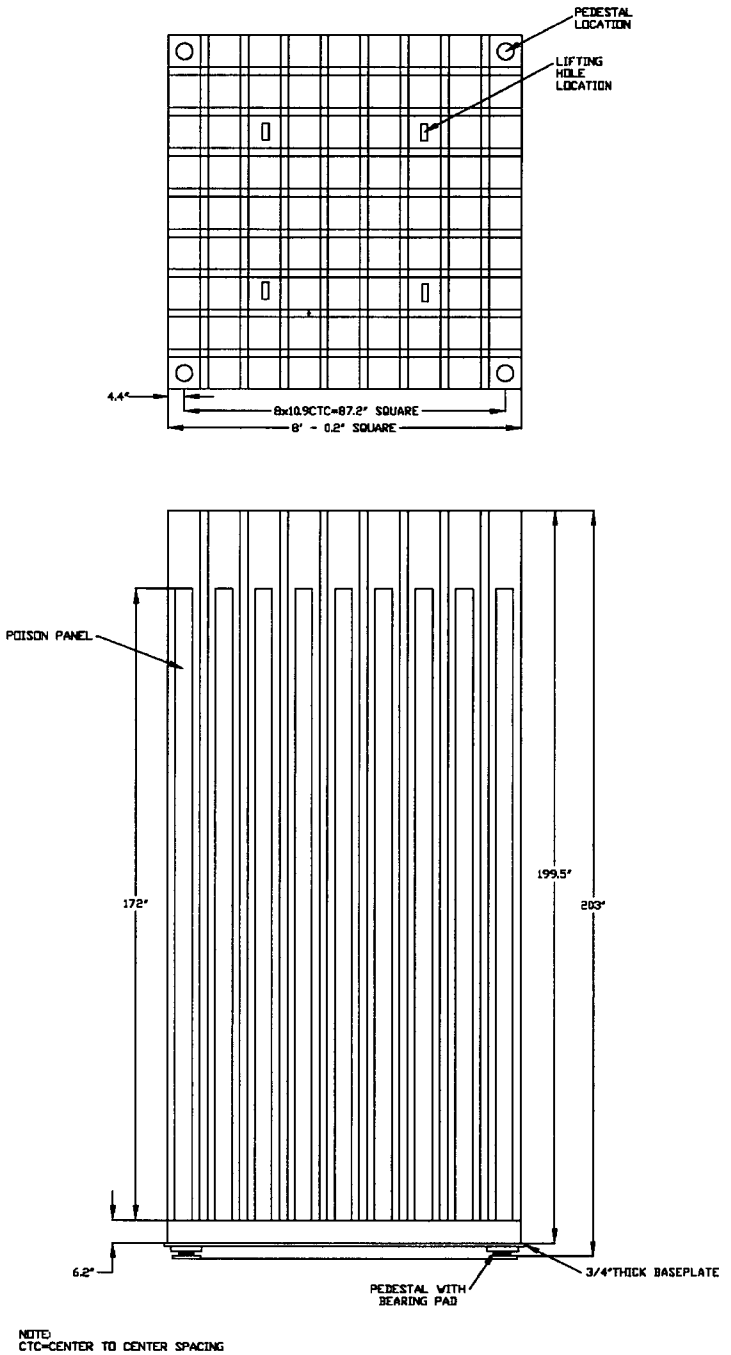

Figure 2-2 Configuration of a Region 1 Storage Cell (Sheet 1 of 2)

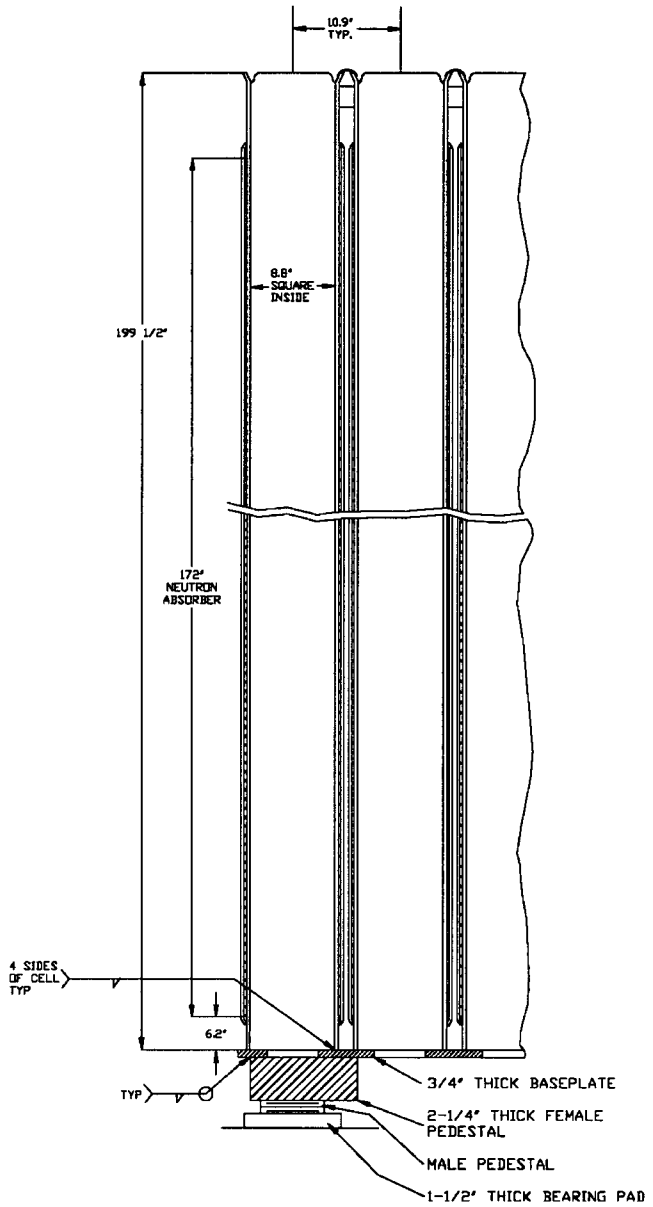

Figure 2-2 Configuration of a Region 1 Storage Cell (Sheet 2 of 2)

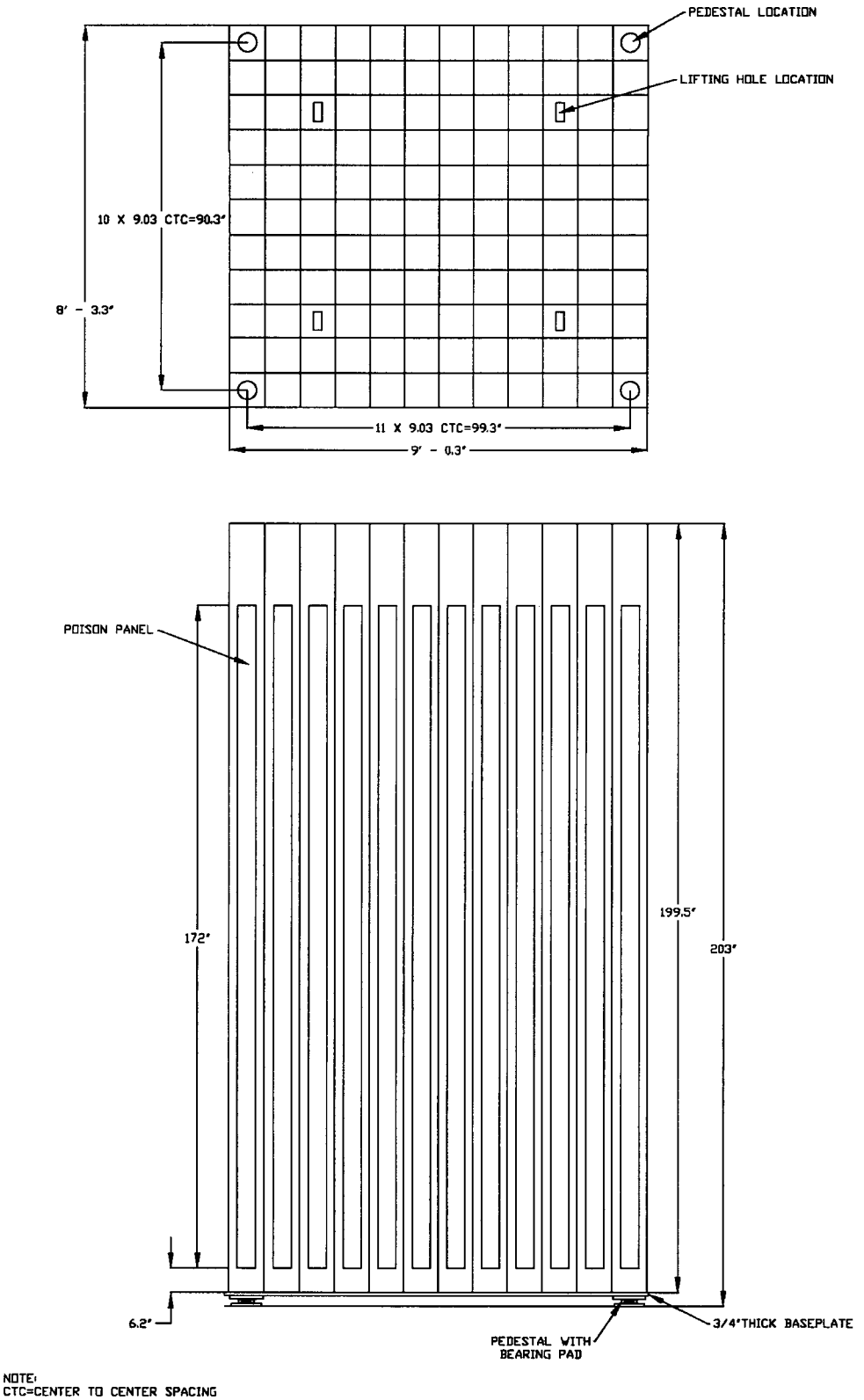

Figure 2-3 Configuration of a Region 2 Storage Cell (Sheet 1 of 2)

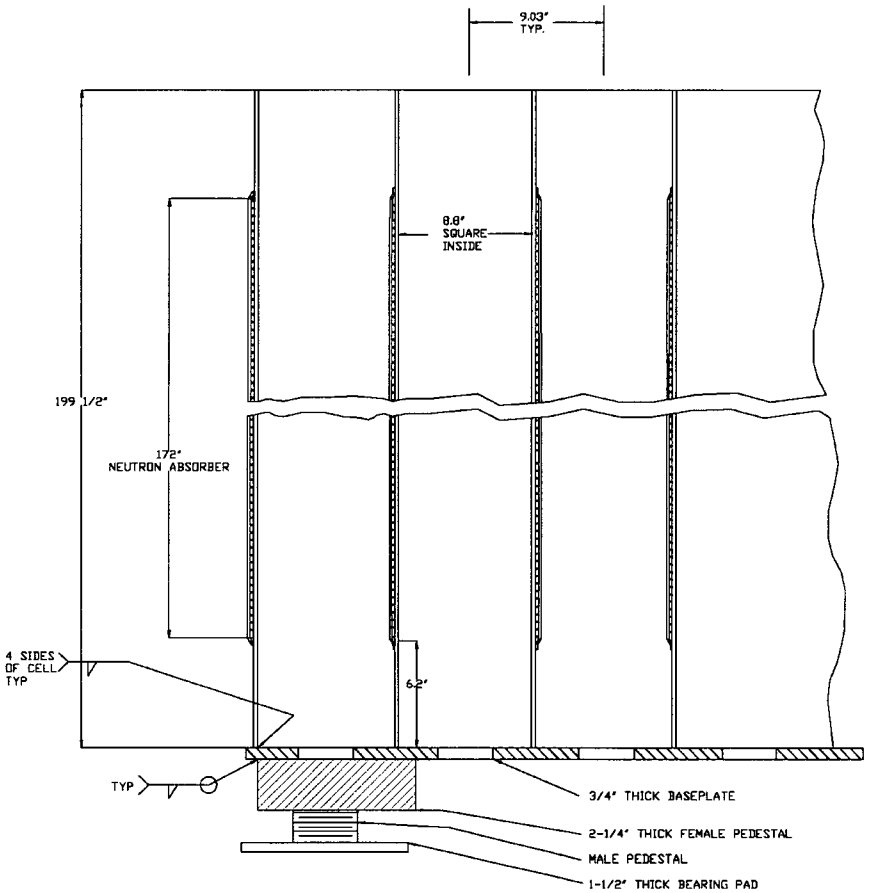

Figure 2-3 Configuration of a Region 2 Storage Cell (Sheet 2 of 2)

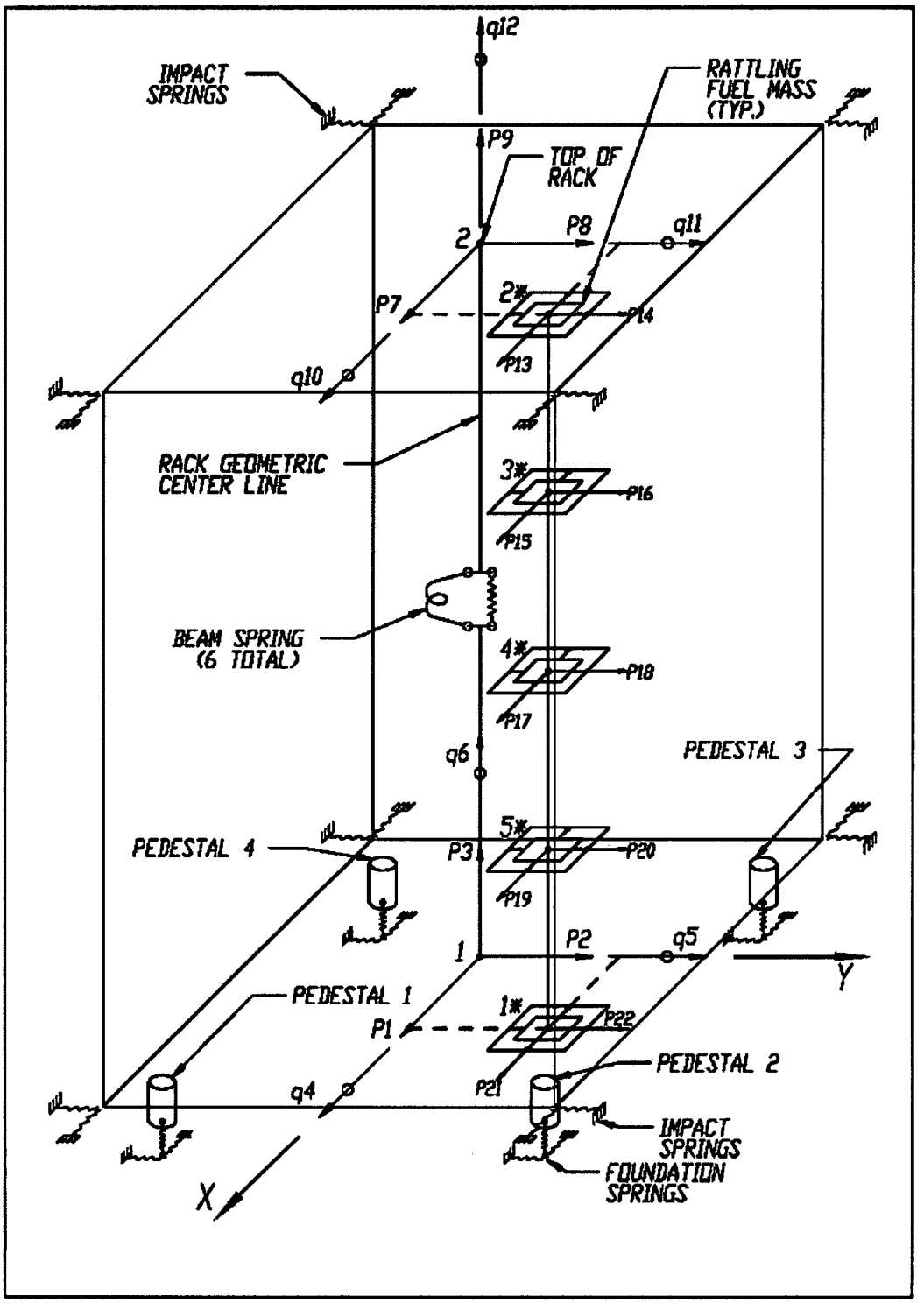

Figure 2-4 Schematic Diagram of Dynamic Model for DYNARACK

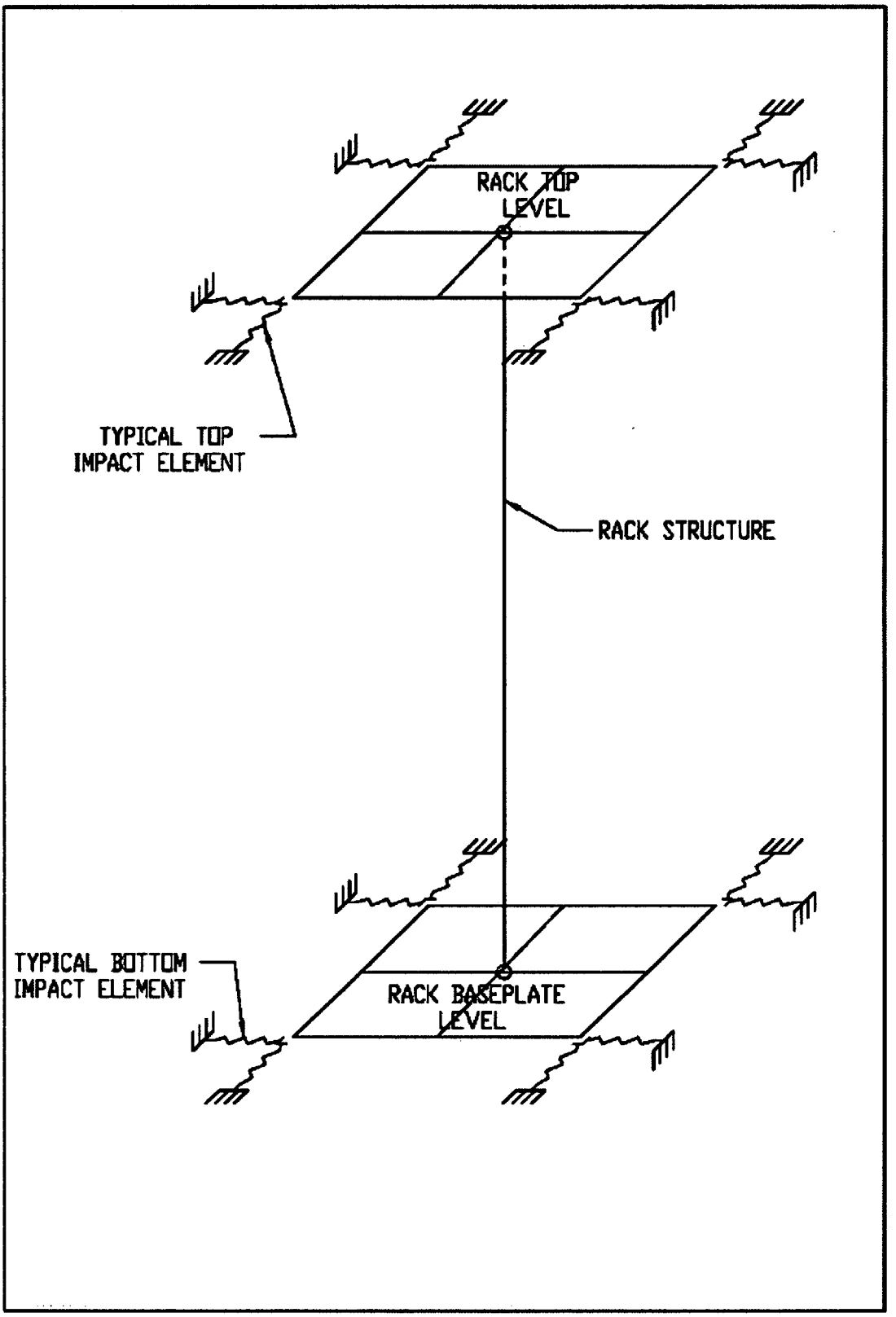

Figure 2-5 Rack-to-Rack Impact Springs

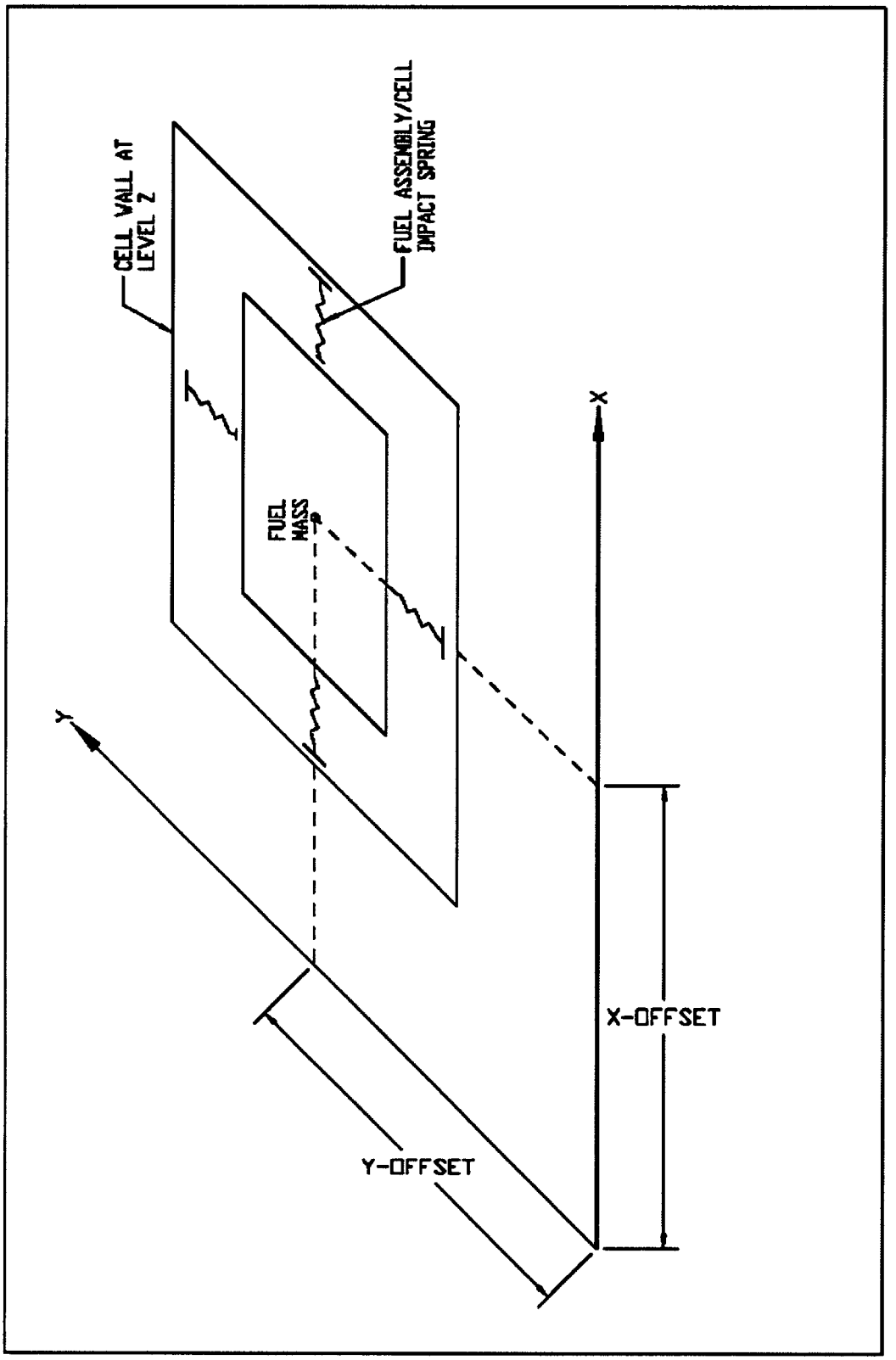

Figure 2-6 Fuel-to-Rack Impact Springs at Level of Rattling Mass

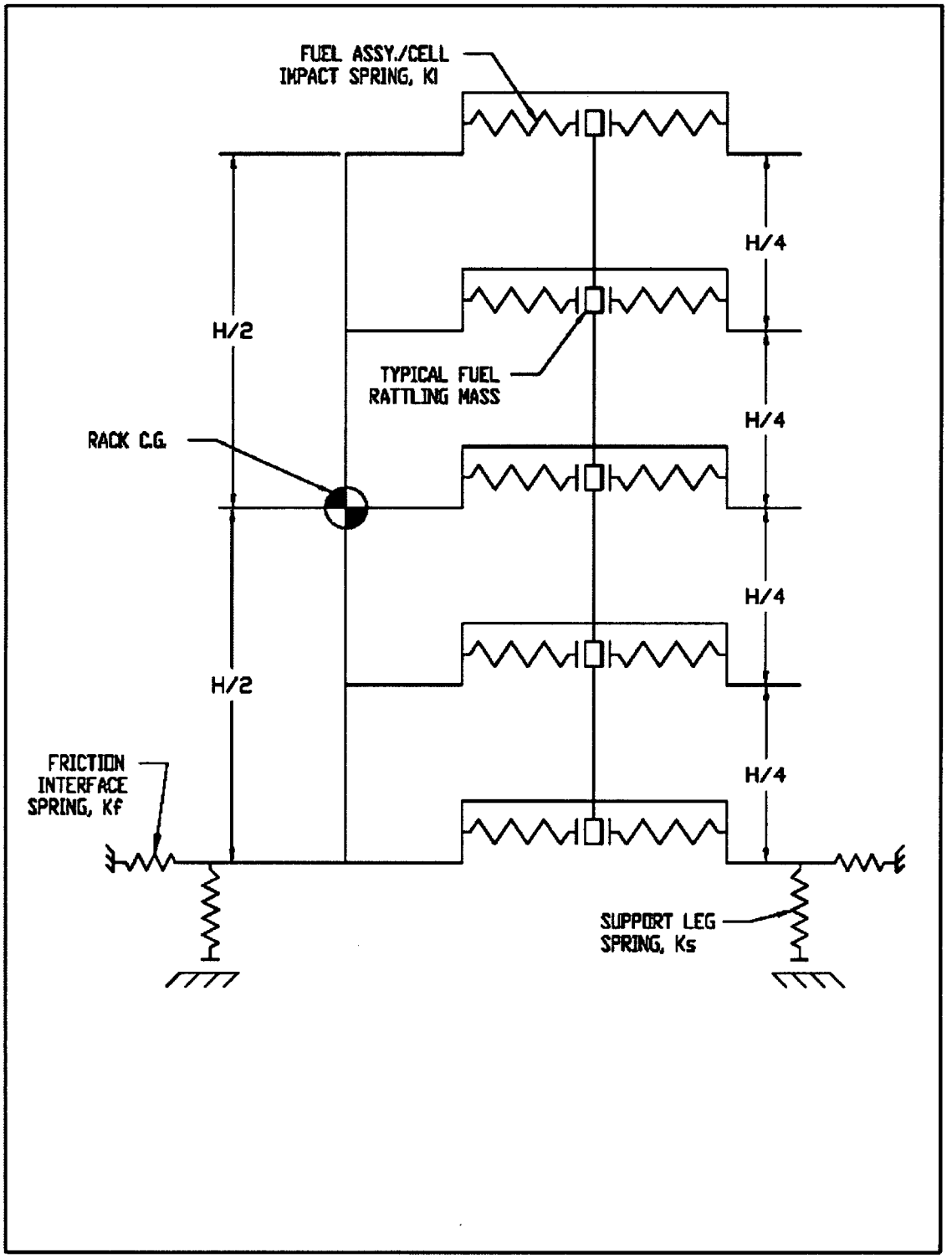

Figure 2-7 Two-Dimensional View of Spring-Mass Simulation

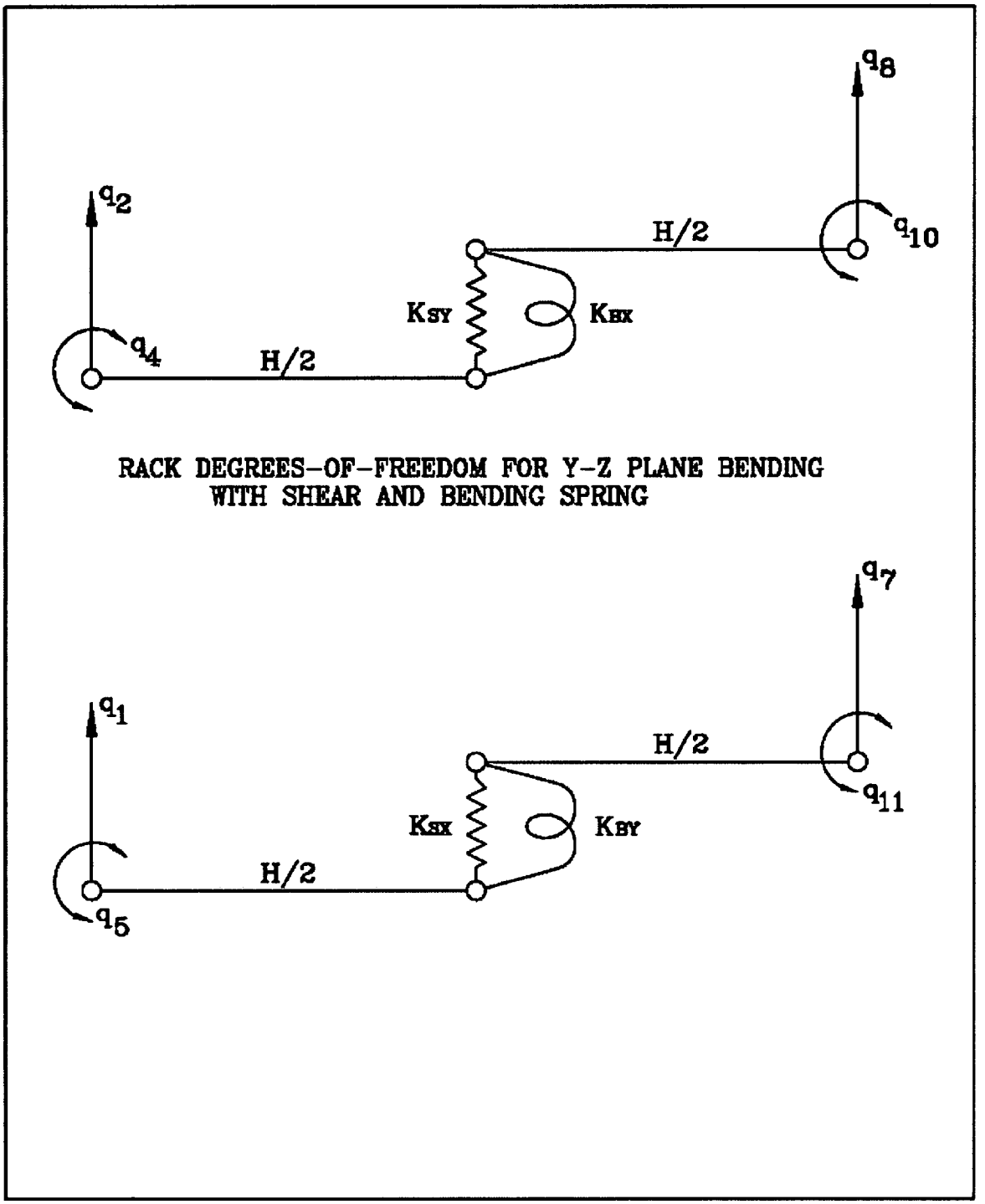

Figure 2-8 Rack Degrees-of-Freedom for X-Y Plane Bending with Shear and Bending Spring

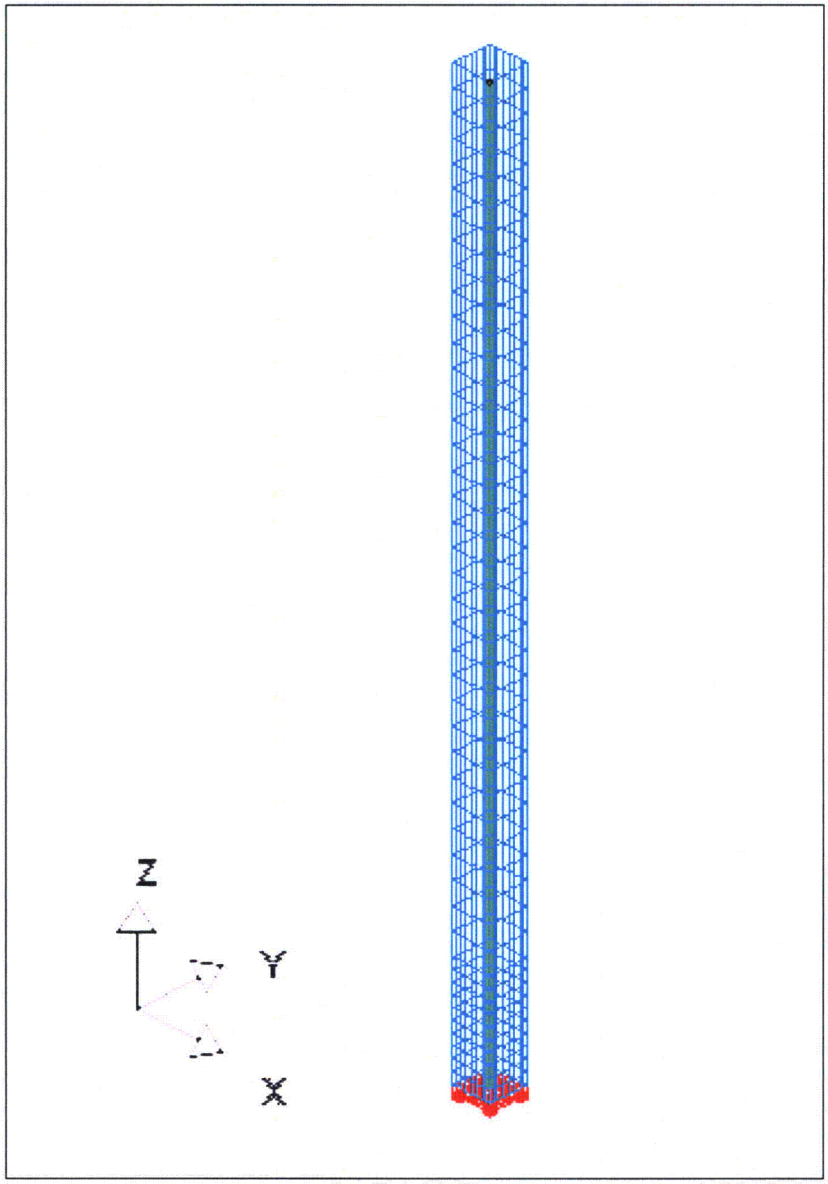

Figure 2-9 LS-DYNA Model of Dropped Fuel Assembly

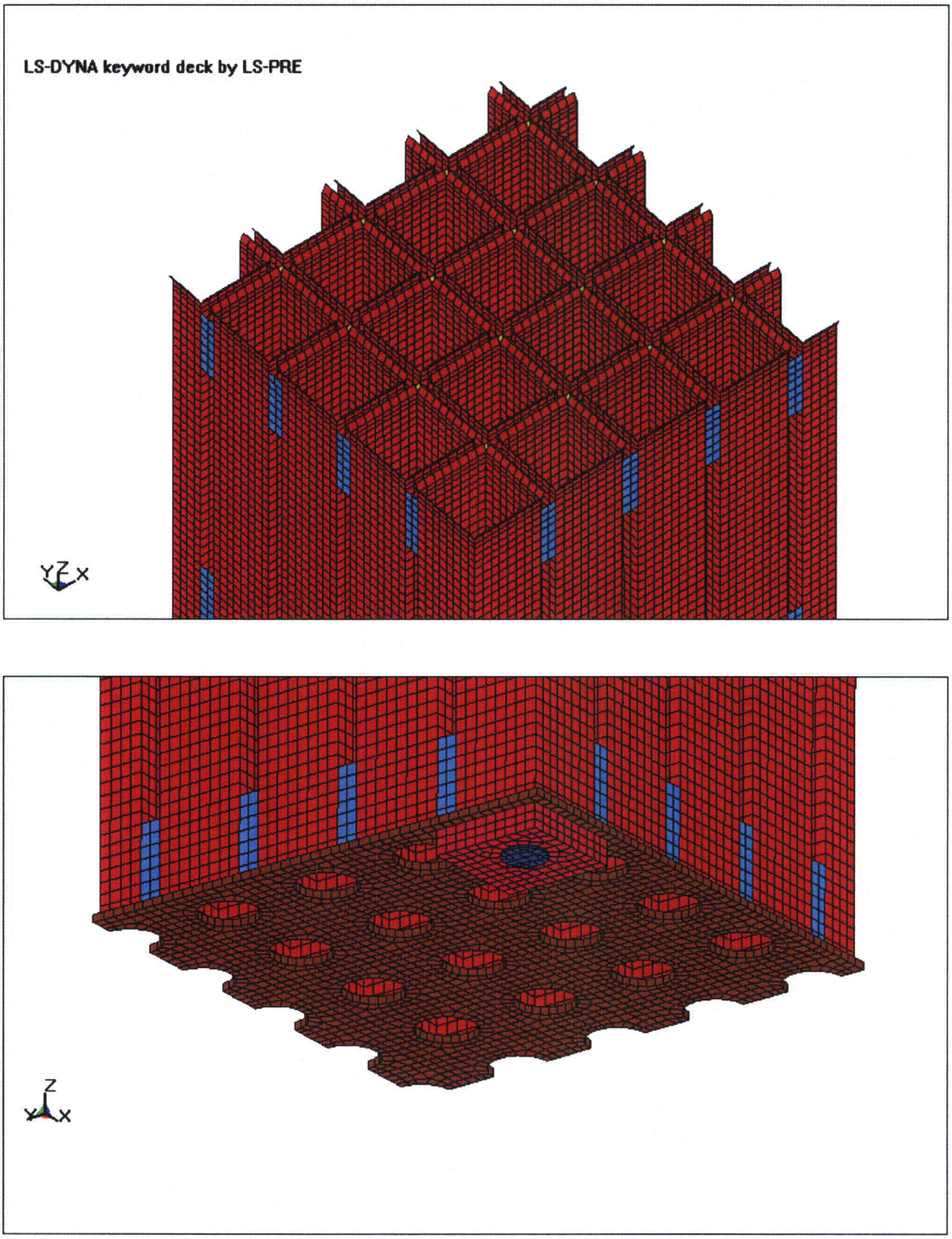

Figure 2-10 LS-DYNA Model of Top and Bottom of AP1000 Region 1 Spent Fuel Rack

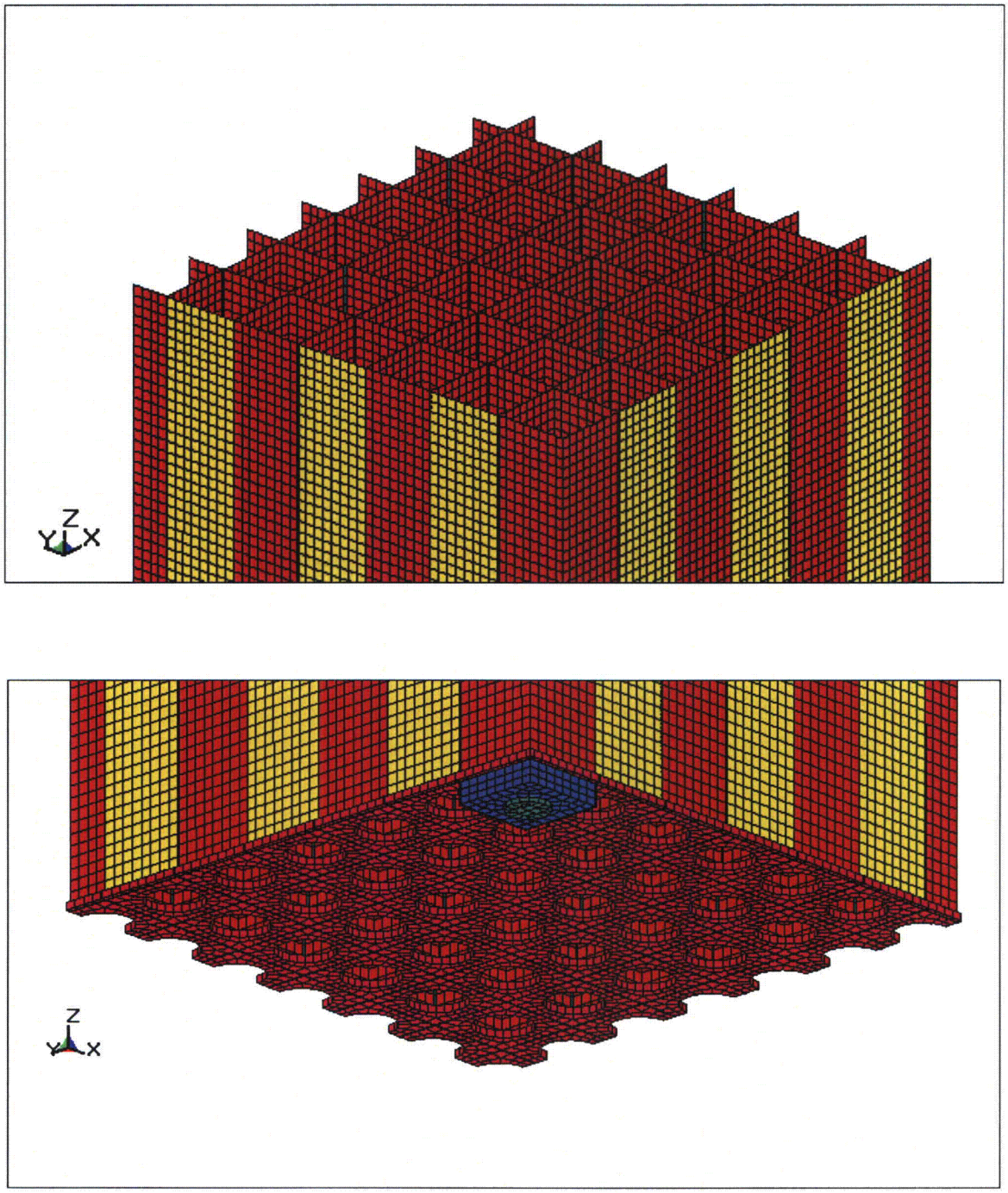

Figure 2-11 LS-DYNA Model of Top and Bottom of AP1000 Region 2 Spent Fuel Rack

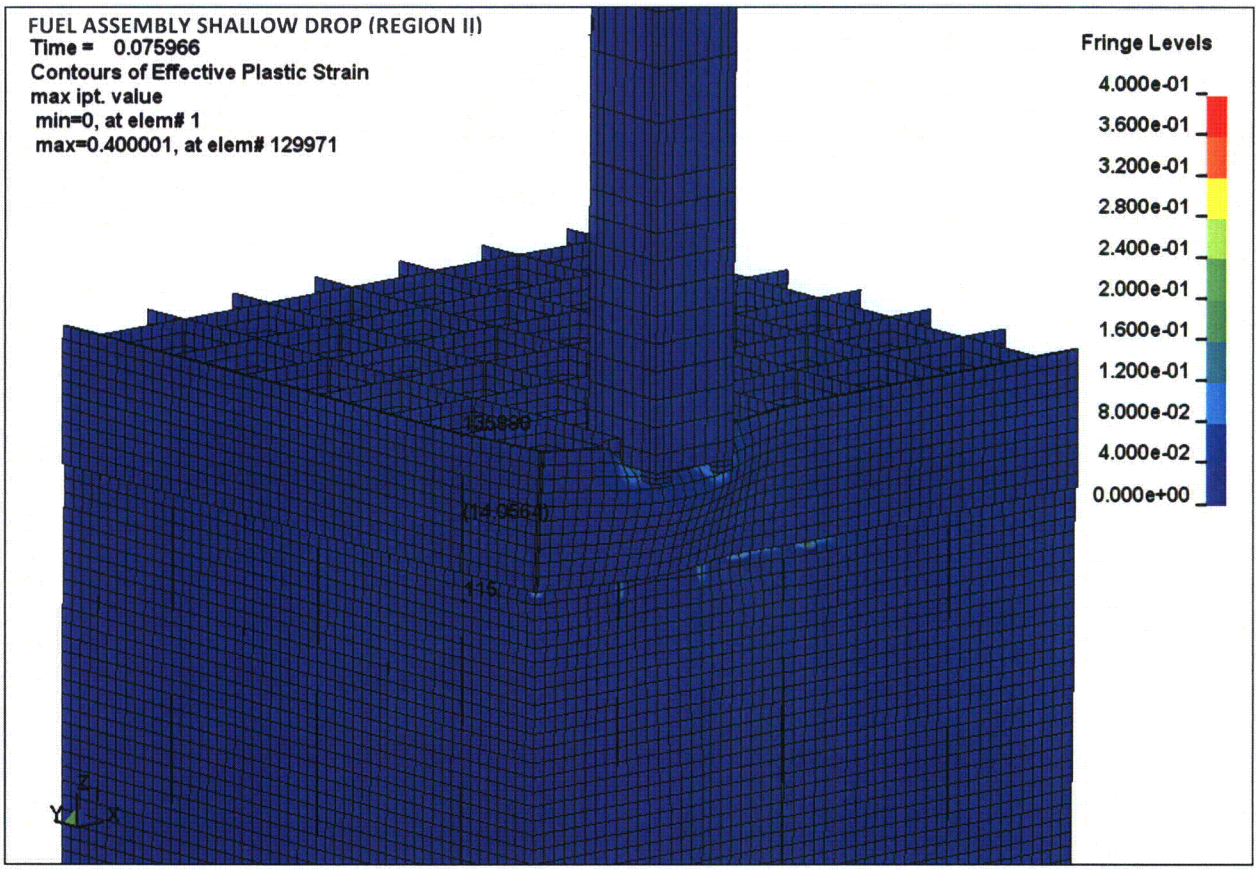

Figure 2-12 Plastic Strain Results from Drop to Top of Region 2 Spent Fuel Rack

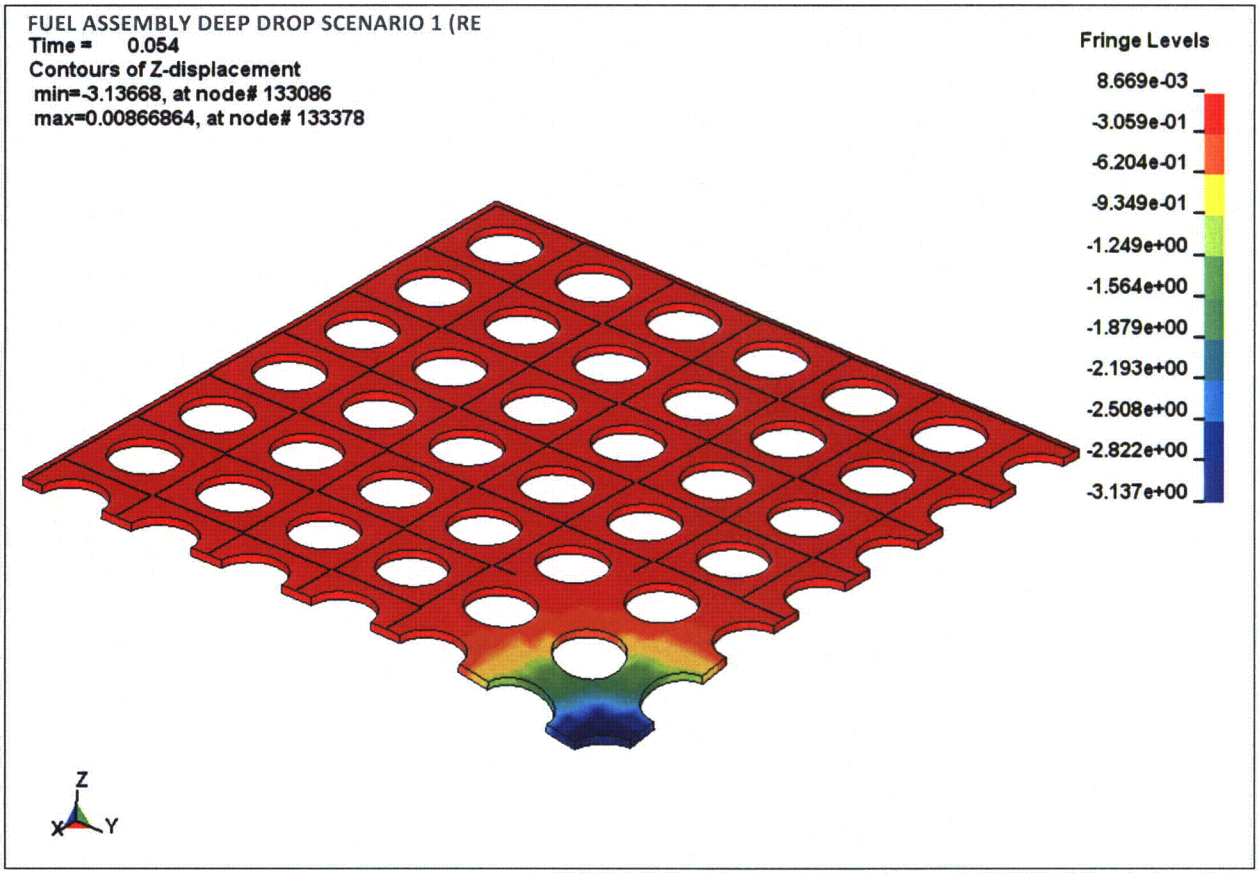

Figure 2-13 Maximum Rack Baseplate Deformation from Drop into an Empty Cell (One-Quarter of Impact Zone Shown)

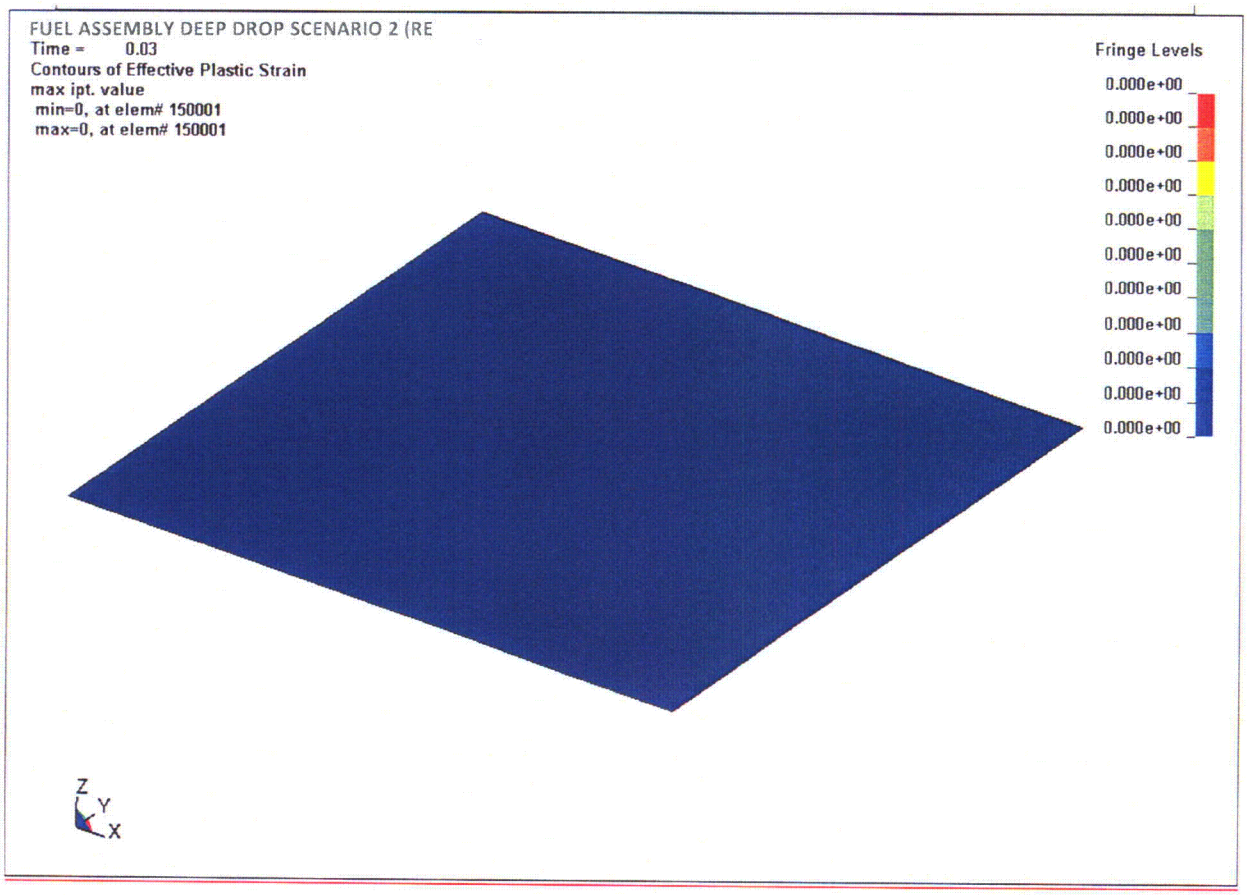

Figure 2-14 Plastic Strain in Pool Liner from Drop over Rack Pedestal

3 REGULATORY IMPACT

The structure/seismic analysis of the AP1000 Spent Fuel Storage Racks is addressed in subsection 9.1.2, "Spent Fuel Storage" of the NRC Final Safety Evaluation Report (Reference 2). The completion of the structural/seismic analysis for the AP1000 Spent Fuel Storage Racks is identified in the Final Safety Evaluation Report as COL Action Item 9.1.6-3.

The changes to the DCD presented in this report do not represent an adverse change to the design functions of the AP1000 Spent Fuel Storage Racks, or to how design functions are performed or controlled. From a thermal perspective, the Spent Fuel Pool Cooling System has the capability to cool the fully loaded spent fuel pool (889 fuel assemblies) under the design-basis conditions. The structural/seismic analysis of the AP1000 Spent Fuel Storage Racks is consistent with the description of the analysis in subsection 9.1.2.2.1, "Spent Fuel Rack Design," of the DCD. Therefore, the changes to the DCD do not involve revising or replacing a DCD-described evaluation methodology. The changes to the DCD do not involve a test or experiment not described in the DCD. The DCD change does not require a license amendment per the criteria of VIII.B.5.b. of Appendix D to 10 CFR Part 52.

None of the changes described involve design features used to mitigate severe accidents. Therefore, a license amendment based on the criteria of VIII.B.5.c of Appendix D to 10 CFR Part 52 is not required.

The closure of the COL Information Item will not alter barriers or alarms that control access to protected areas of the plant. The closure of the COL Information Item will not alter requirements for security personnel. Therefore, the closure of the COL Information Item does not have an adverse impact on the security assessment of the AP1000.

4 REFERENCES

1. APP-GW-GL-700, AP1000 Design Control Document, Rev. 16.

2. Final Safety Evaluation Report Related to Certification of the AP1000 Standard Design, September 2004.

3. Westinghouse Calculation, APP-FS02-S3C-002 Rev. 0, "AP1000 Spent Fuel Storage Racks Structural/Seismic Analysis," June 2006. (Westinghouse Proprietary)

4. AP1000 Standard Combined License Technical Report, APP-GW-GLR-030, Rev. 0, "Spent Fuel Storage Racks Design Criticality Analysis," June 2006.

5. "U.S. NRC OT Position for Review and Acceptance of Spent Fuel Storage and Handling Applications," GL 78-11 April 14, 1978, and GL 79-04 January 18, 1979, amendment.

6. U.S. NRC Standard Review Plan, NUREG-0800 (SRP 3.8.4, Rev 1).

7. Paul, B., "Fluid Coupling in Fuel Racks: Correlation of Theory and Experiment," NUSCO/Holtec Report HI-88243. (Holtec Proprietary)

8. U.S. NRC Standard Review Plan, NUREG-0800 (SRP 3.7.1, Rev. 2).

9. Holtec Drawing No. 4743, "Discrete Zone Two Region Spent Fuel Rack Pool Layout," Rev. 0, June 2006. (Holtec Proprietary)

10. Soler, A.I. and Singh, K.P., "Seismic Responses of Free Standing Fuel Rack Constructions to 3-D Motions," Nuclear Engineering and Design, Vol. 80, pp. 315-329 (1984).

11. Levy, S., and Wilkinson, John, "The Component Element Method in Dynamics," McGraw Hill, 1976.

12. ASME Boiler & Pressure Vessel Code Section III, Subsection NF, 1998 edition with 2000 addenda.

13. Holtec Computer Code MR216 (multi-rack transient analysis code, a.k.a. DYNARACK), Version 2.00. QA documentation contained in Holtec Report HI-92844. (Holtec Proprietary)

14. ASME Boiler & Pressure Vessel Code, Section II, Part D, 1998 edition with 2000 addenda.

15. Holtec Computer Code DYNAPOST (Analysis Post Processor), v. 2.0. (Holtec Proprietary)

16. Fritz, R.J., "The Effects of Liquids on the Dynamic Motions of Immersed Solids," Journal of Engineering for Industry, Trans. of the ASME, February 1972, pp. 167-172.

17. "Strength of Materials," S.P. Timoshenko, 3rd Edition, Part II, pp194-197 (1956).

18. Deleted

19. AP1000 Letter Number DCP/HII0005, from J.M. Iacovino (Westinghouse Electric Company) to Mr. Eric Bush (Holtec International), Dated March 27, 2006. (Westinghouse Proprietary)

20. Rack Data Sheet AP1000, Rev. 5., Holtec International, June 2006. (Holtec Proprietary)

21. Rabinowicz, E., "Friction Coefficients of Water Lubricated Stainless Steels for a Spent Fuel Rack Facility," MIT, a report for Boston Edison Company, 1976.

22. Westinghouse Document No: APP-GW-G1-003, "AP1000 Seismic Design Criteria," Rev. 0, July 2002. (Westinghouse Proprietary)

23. Holtec Report HI-2063492, "New Fuel Rack Structural/Seismic Analysis for Westinghouse AP1000," Rev. 0., Project 1540, May 2006. (Holtec Proprietary)

24. LS-DYNA, v970 Livermore Software Technology Corporation, 2005.

25. Timoshenko and Gere, "Theory of Elastic Stability," McGraw-Hill, Second Edition, 1961.

26. ASME Boiler & Pressure Vessel Code, Section III, Appendices, 1998 Edition with 2000 Addenda.

27. Westinghouse Calculation, APP-1230-CAC-001, Revision 1, "Design of Spent Fuel Pit Floor in Module CA20," December 2007. (Westinghouse Proprietary)

28. U.S. NRC, Regulatory Guide 1.124, Revision 1, "Service Limits and Loading Combinations for Class 1 Linear-Type Component Supports," January 1978.

5 DCD MARKUP

The following markup to Revision 16 of the DCD identifies how COL application FSARs should be prepared to incorporate the subject change. Revision 1 of APP-GW-GLR-033 markups of the DCD will be incorporated into a future revision of the DCD.

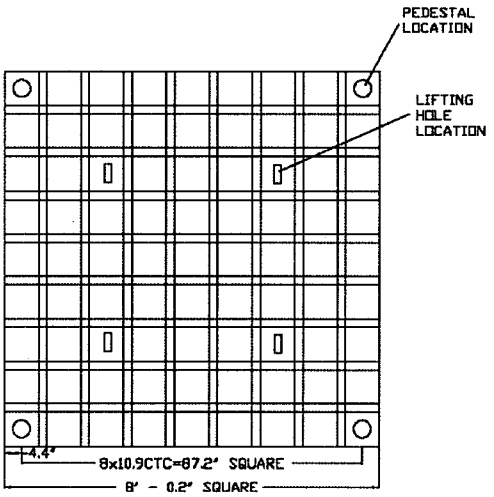

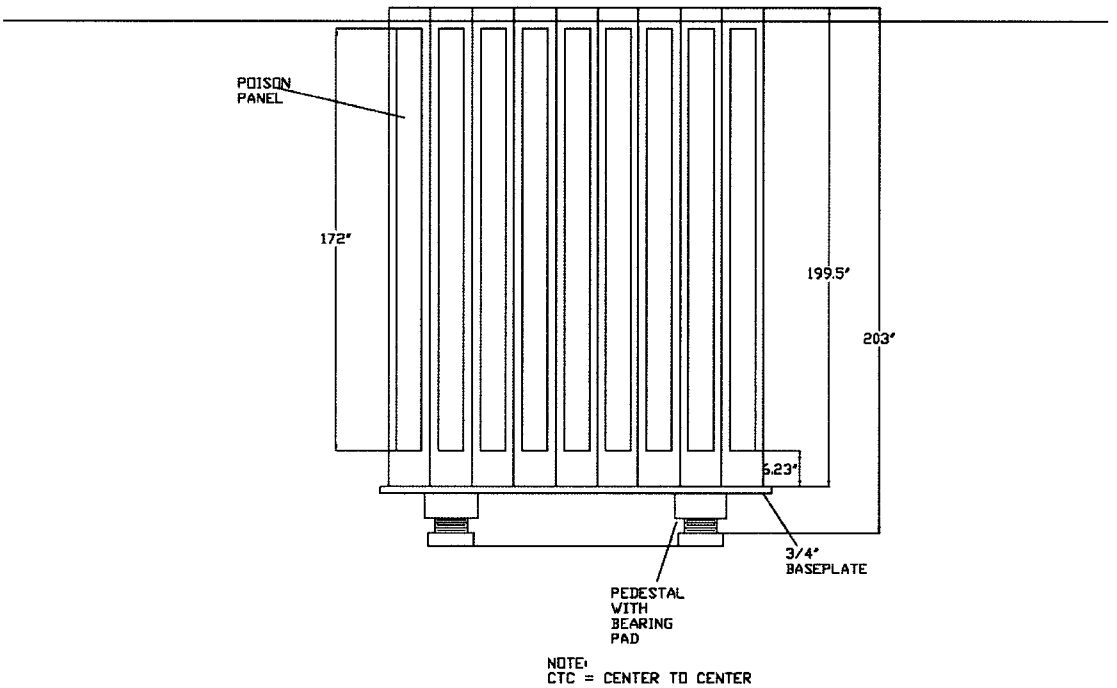

~~Figure 9.1-2 (Sheet 1 of 2)~~

~~Region 1 Spent Fuel Storage Rack Layout~~

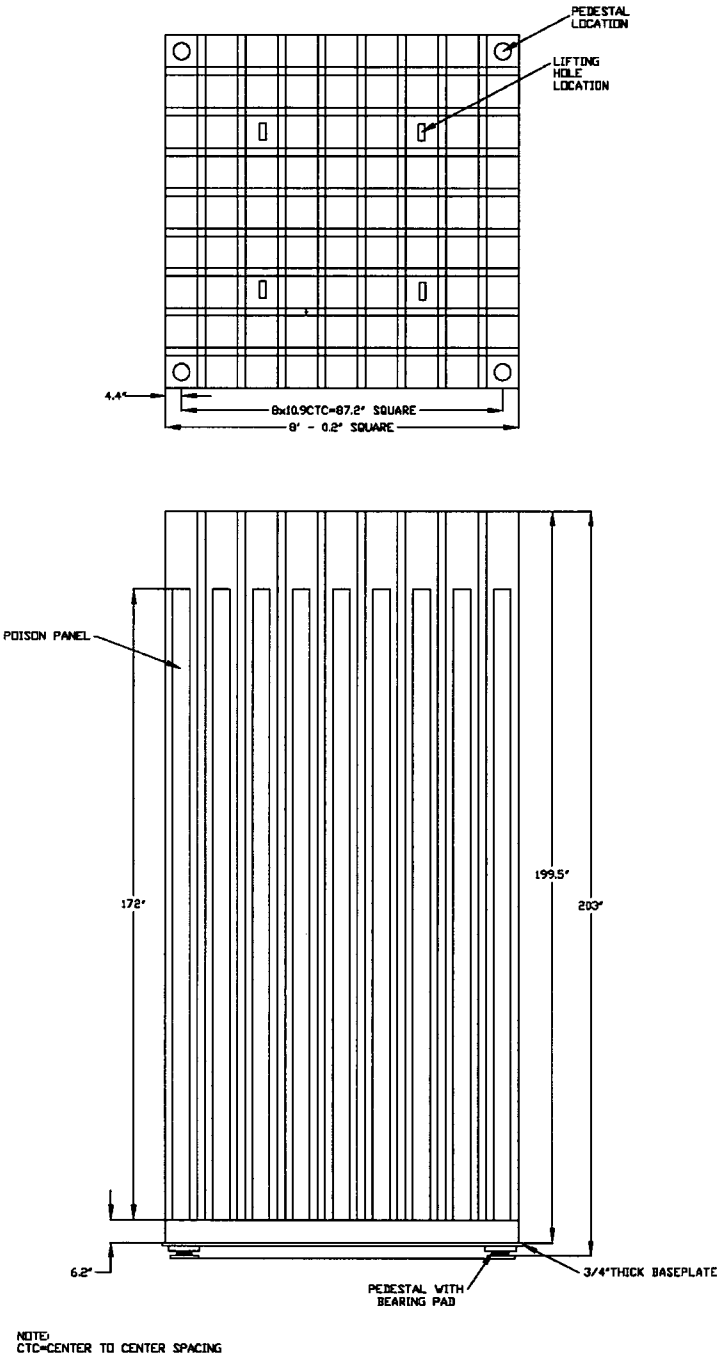

Figure 9.1-2 (Sheet 1 of 2)

Region 1 Spent Fuel Storage Rack Layout

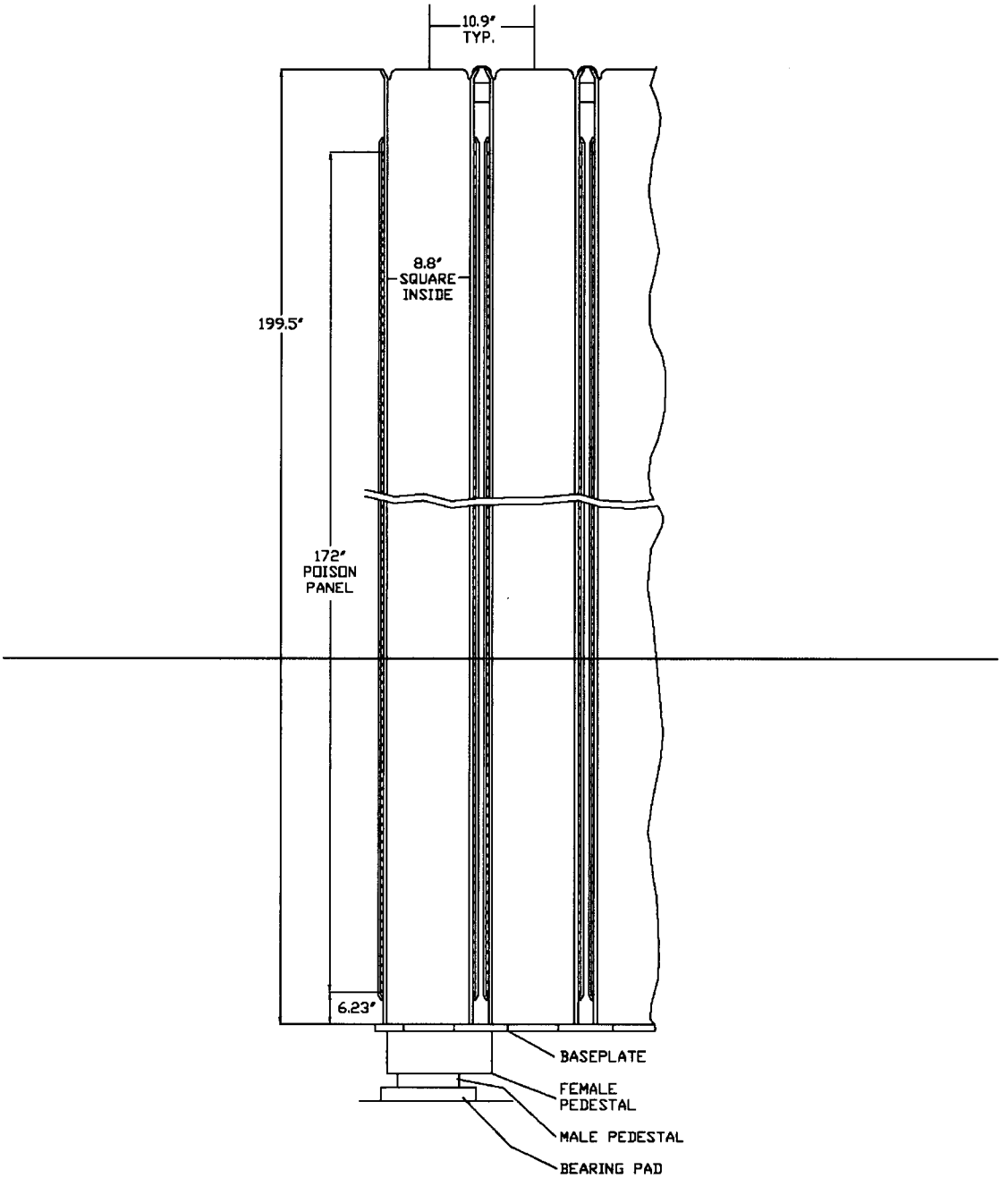

~~Figure 9.1-2 (Sheet 2 of 2)~~

~~**Region 1 Spent Fuel Storage Rack Cross Section**~~

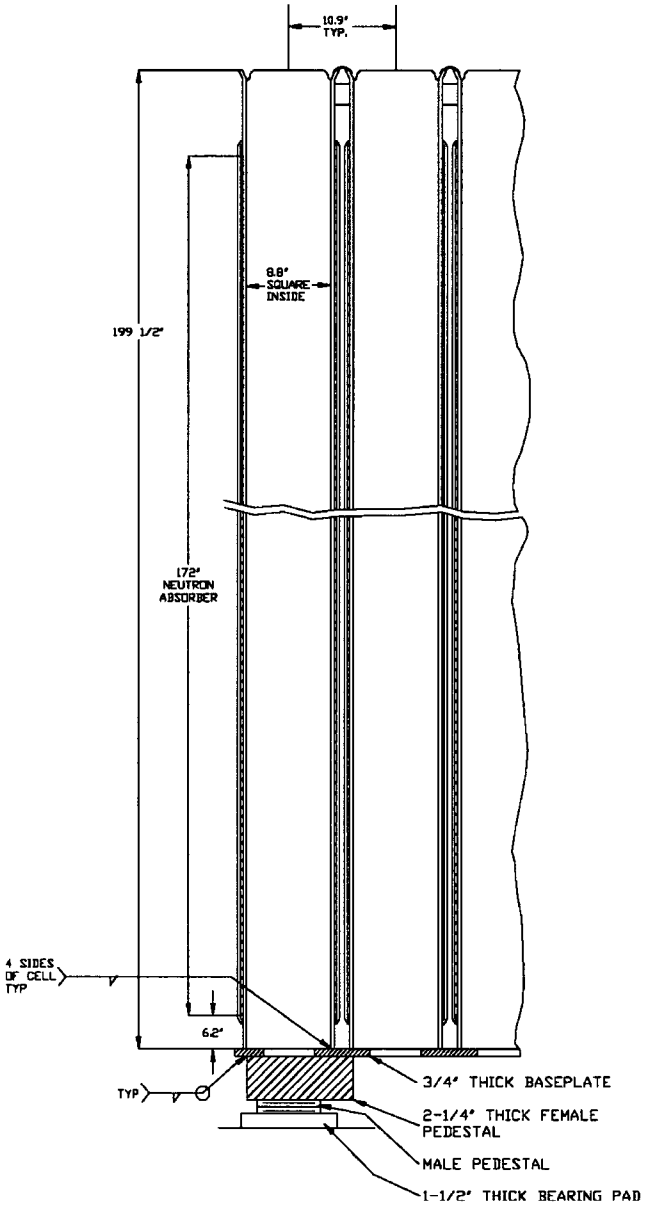

Figure 9.1-2 (Sheet 2 of 2)

Region 1 Spent Fuel Storage Rack ~~Layout~~ Cross Section

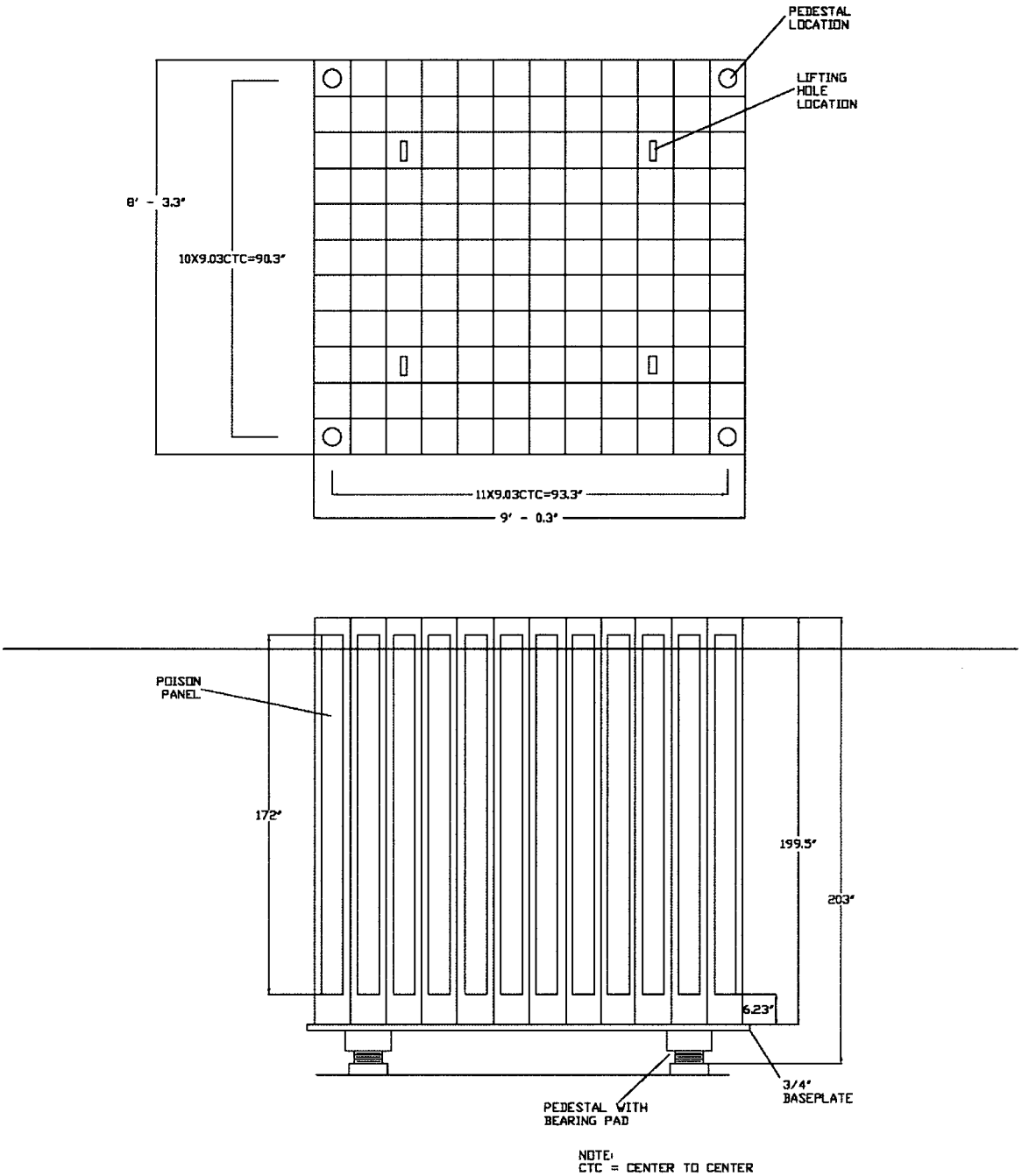

~~Figure 9.1-3 (Sheet 1 of 2)~~

~~Region 2 Spent Fuel Storage Rack Layout~~

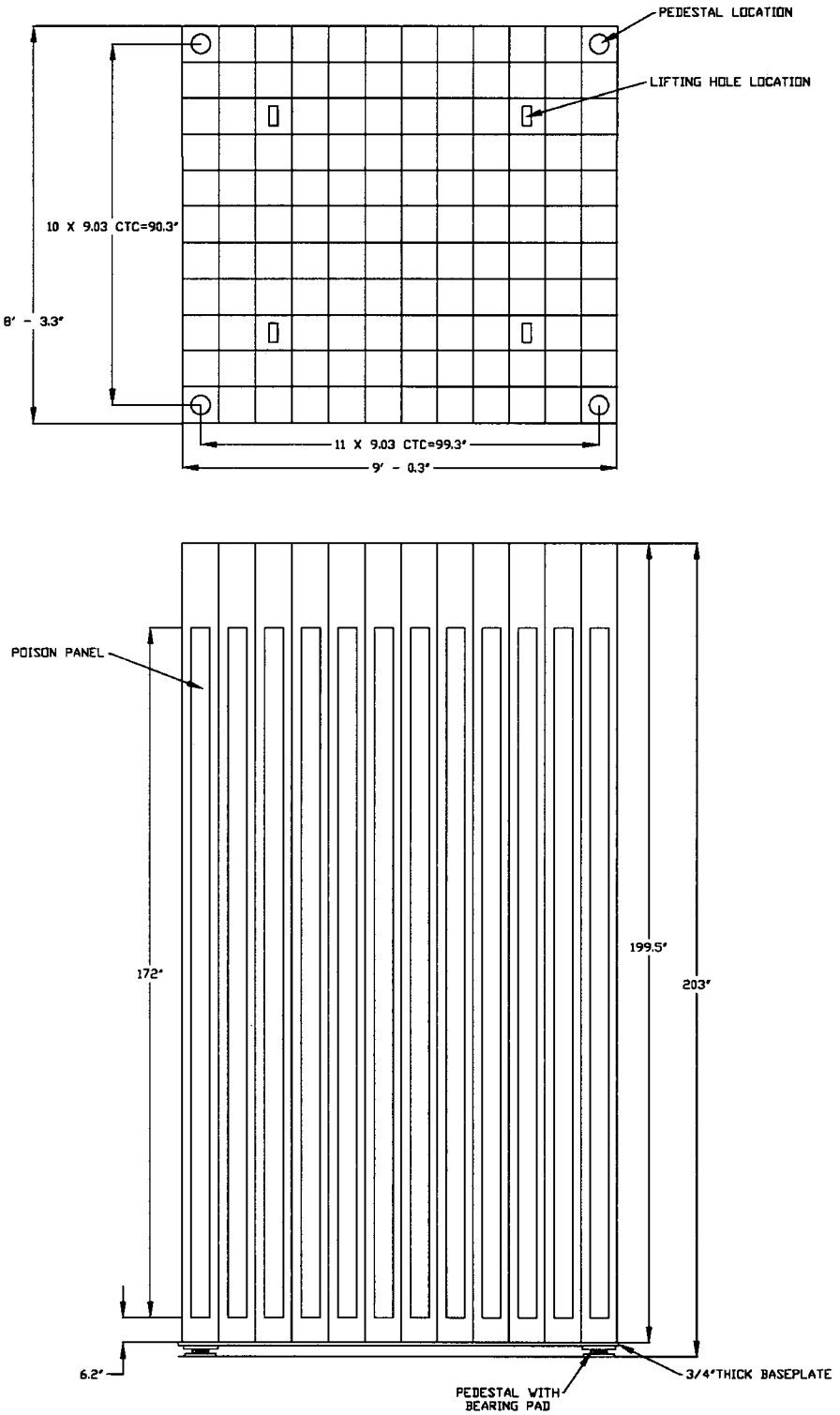

Figure 9.1-3 (Sheet 1 of 2)

Region 2 Spent Fuel Storage Rack Layout

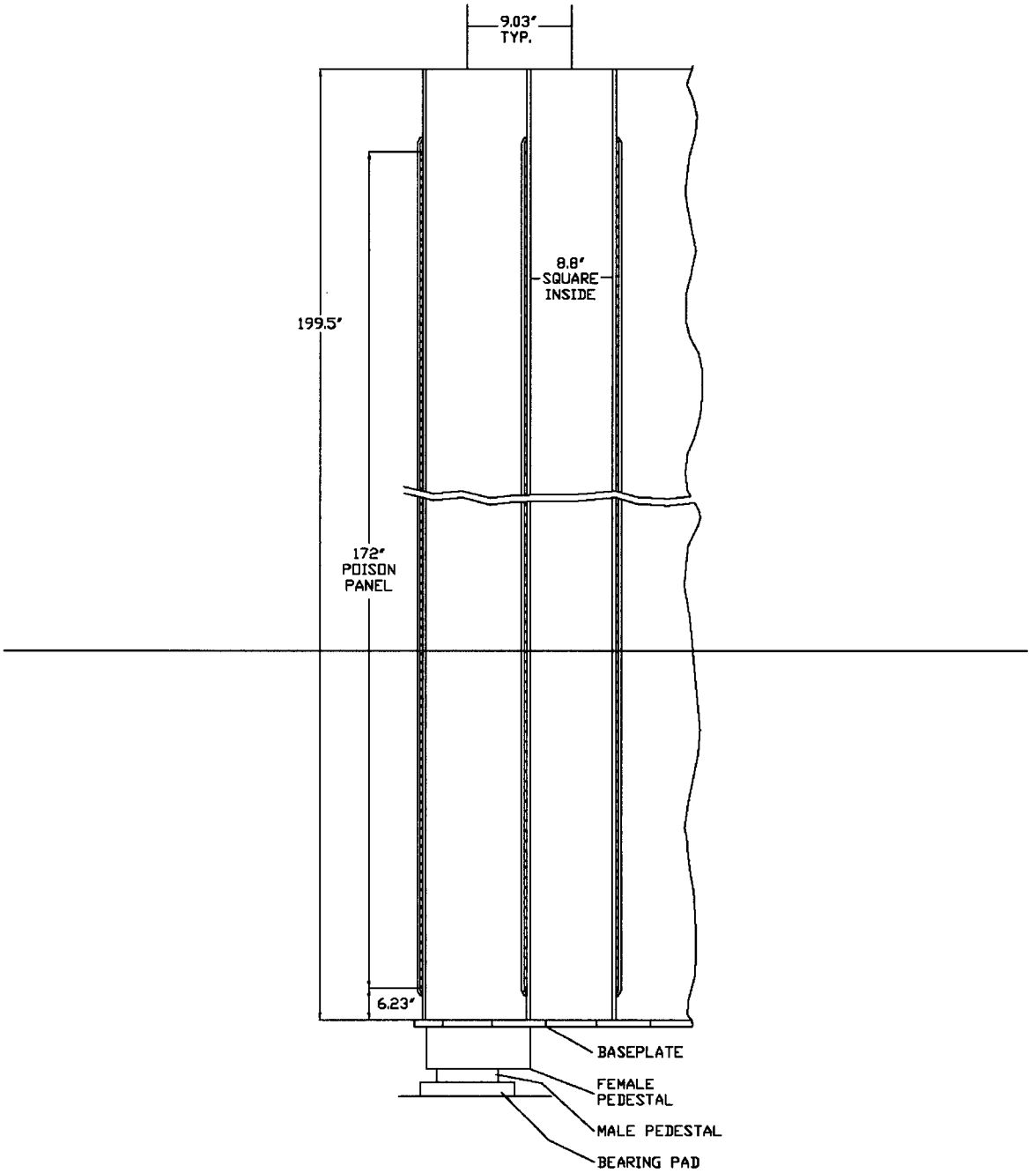

~~Figure 9.1-3 (Sheet 2 of 2)~~

~~**Region 2 Spent Fuel Storage Rack Cross Section**~~

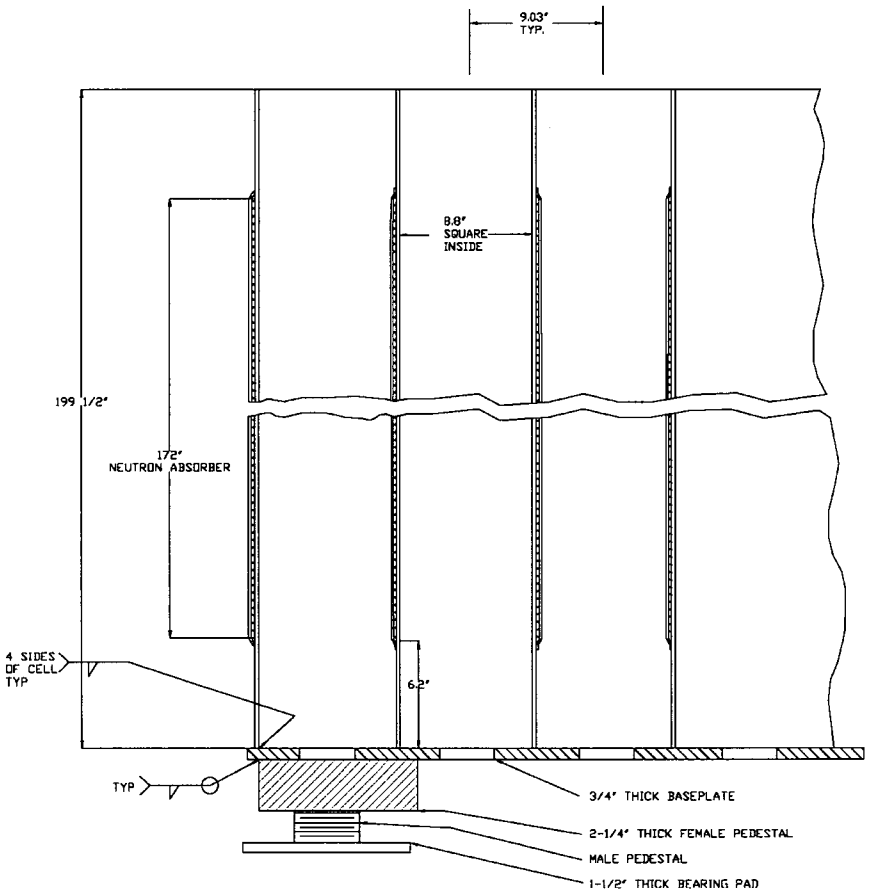

Figure 9.1-3 (Sheet 2 of 2)

Region 2 Spent Fuel Storage Rack Cross Section

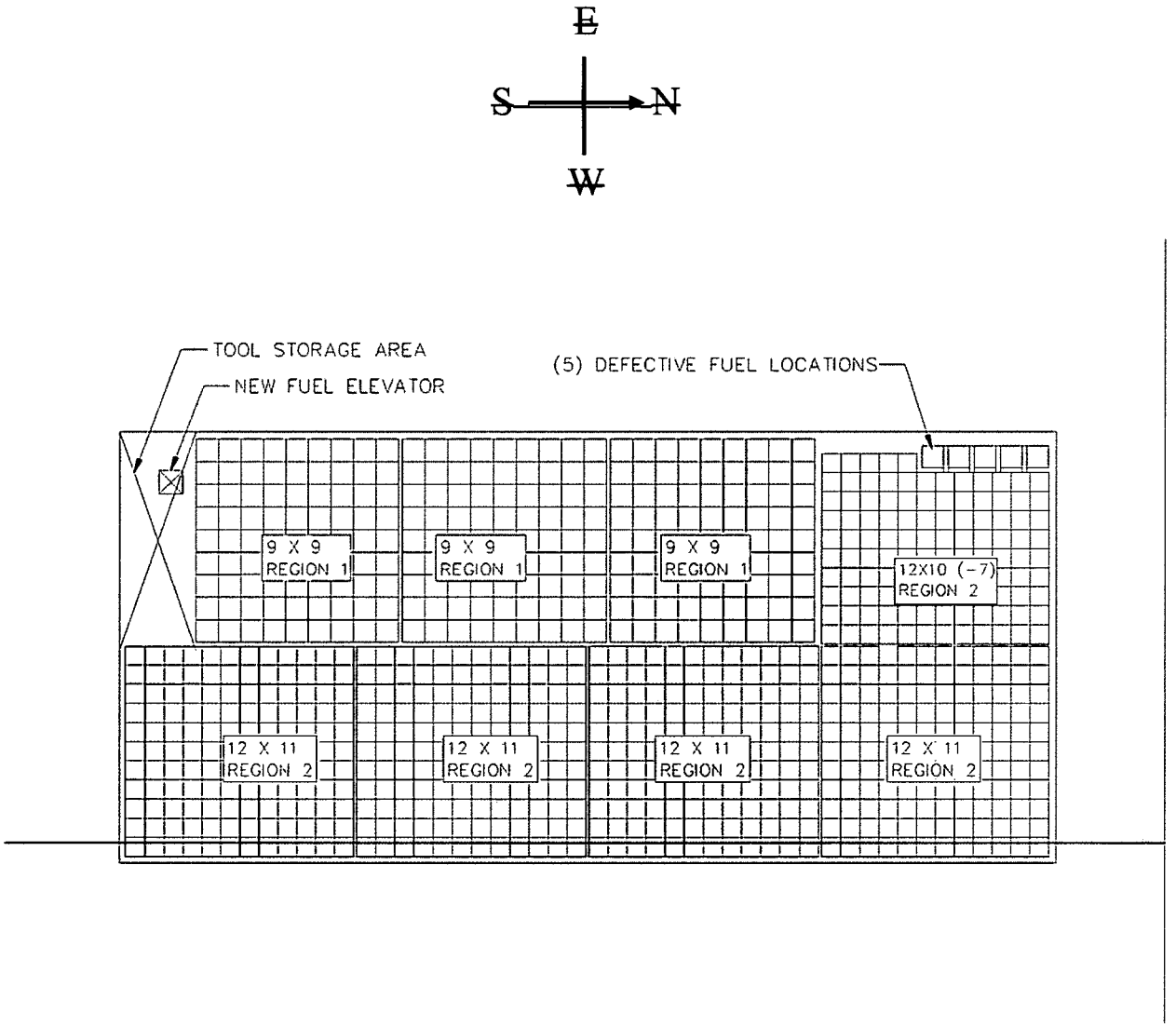

~~Figure 9.1-4~~

~~Spent Fuel Storage Pool Layout (889 Storage Locations)~~

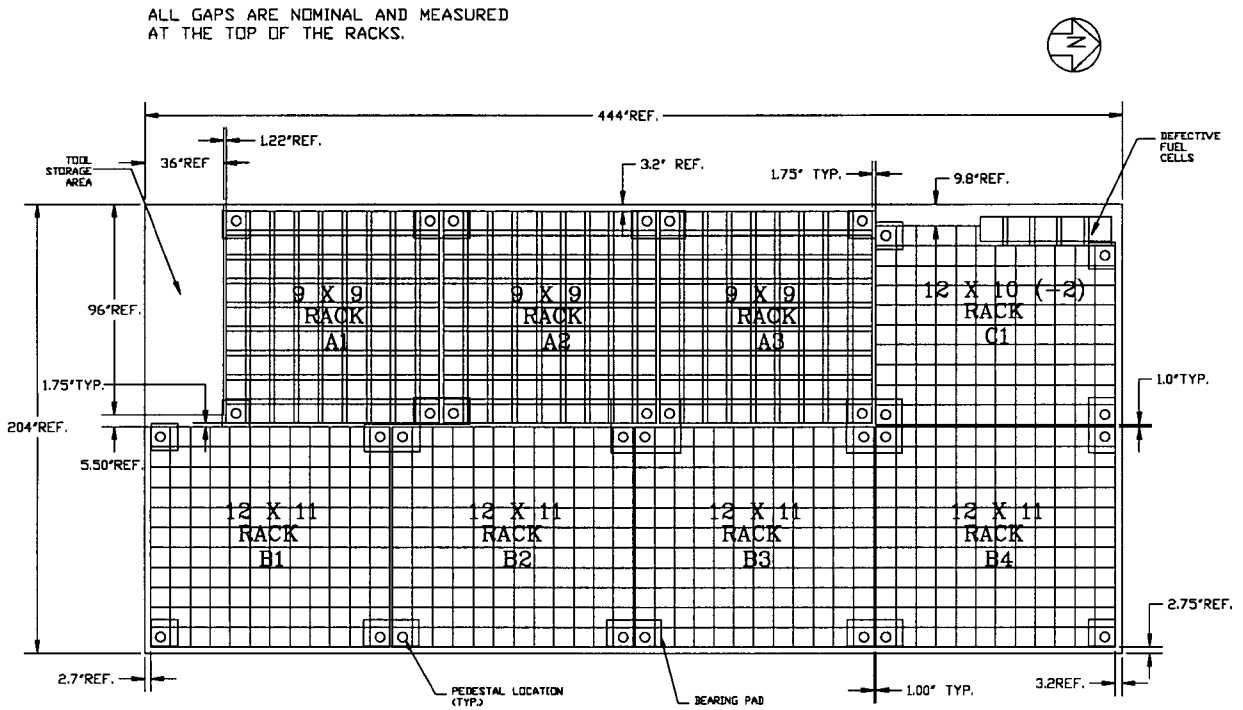

DISCRETE ZONE TWO REGION SPENT FUEL POOL RACK LAYOUT

Figure 9.1-4

Spent Fuel Storage Pool Layout (889 Storage Locations)